Mantle melting trend to high-SiO_2 - low FeO^*/MgO is controlled by the reaction relation oliv + liq → opx.

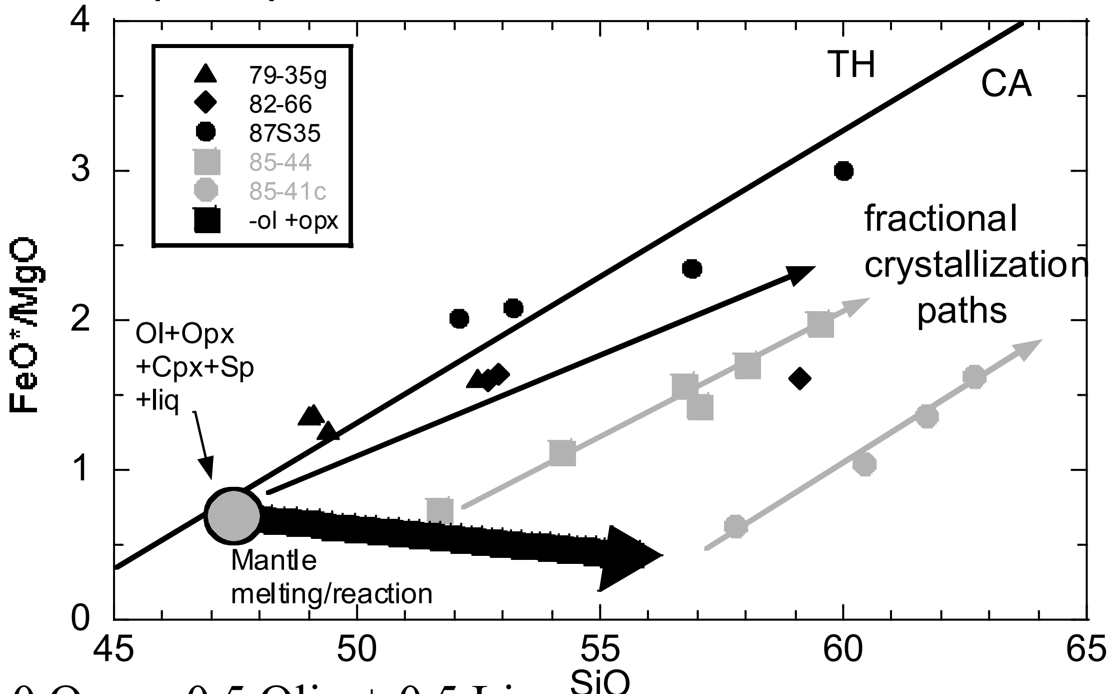

$$1.0\ Opx = 0.5\ Oliv + 0.5\ Liq$$

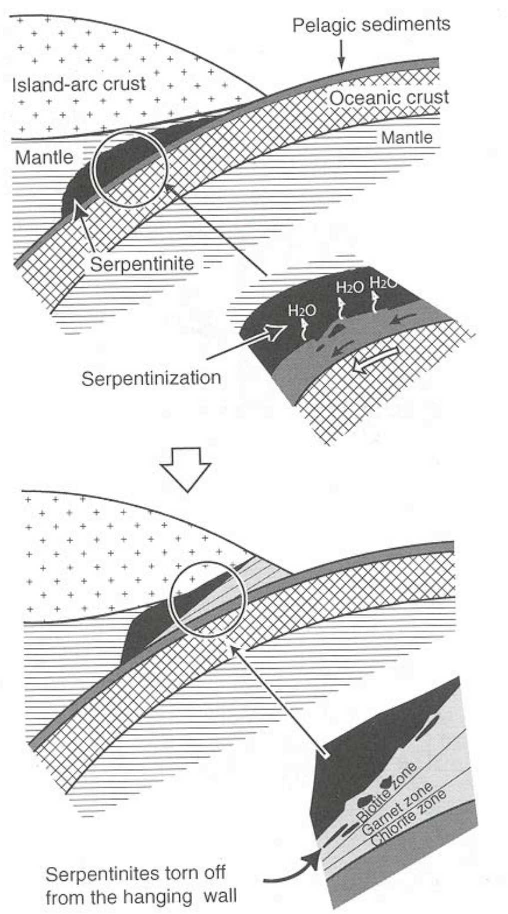

Structural and metamorphic studies of exhumed high pressure subduction complexes (Enami et al., 2004; Maekawa et al., 2004; Kombayashi, 2004) show:

Serpentinites were formed in the mantle wedge above the subducted plate.

These were transported to depth in the subduction zone along with the sediments and basalts associated with the slab.

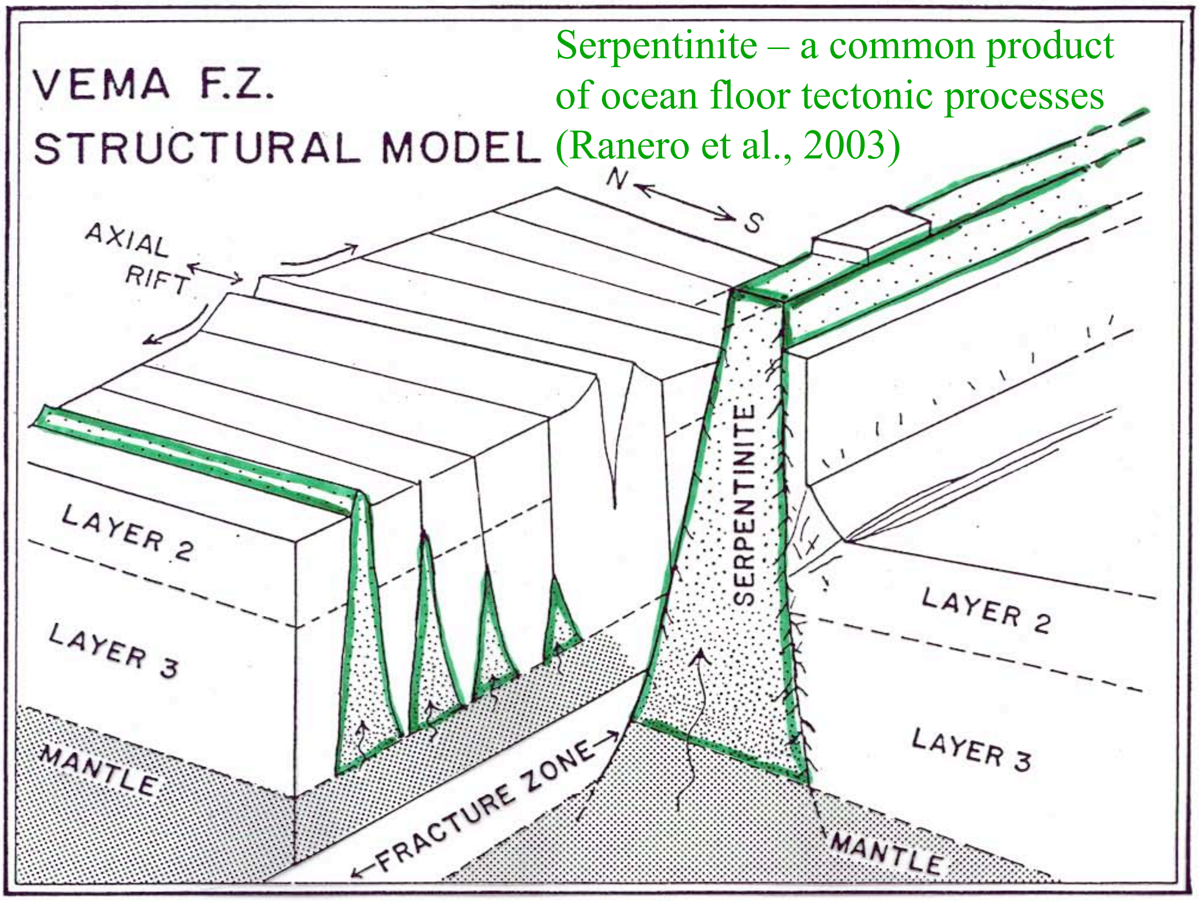

Experimental Details

Au capsules – Piston cylinder - 1.2 – 3.2 GPa
Hart & Zindler Primitive Mantle
Oxide starting mix
With MgO added as $Mg(OH)_2$ = 14 wt. % H_2O

Run Duration

96 – 140 hours (a few at 24 hrs)

Experimental Products

Homogeneous olivine, opx, cpx, spinel and/or garnet
Melt or vapor phase (supercritical fluid)

Equilibrium

QUILF used to check Temp. from Opx-Cpx – within 1 sigma of uncertainty
and f_{O2} from oliv-opx-spinel (Ballhaus et al., 1994) =QFM + 0.8

PREVIOUS STUDIES

Run Times	*H_2O added*	*Capsule*
High – T melting		
Kushiro et al. (1968)		
5 – 30 min	*30%*	*Mo & Pt*
Millhollen et al. (1974)		
0.5 – 3 hrs.	*5.7 %*	*Pt*
Green (1973)		
1 – 6 hrs.	*10 %*	*AgPd alloy*
Low – T melting		
Mysen and Boettcher (1975)		
24 – 64 hrs.	*20- 30 %*	*AgPd alloy*
THIS STUDY		
48 – 120 hrs	*14 –30 %*	*Au*

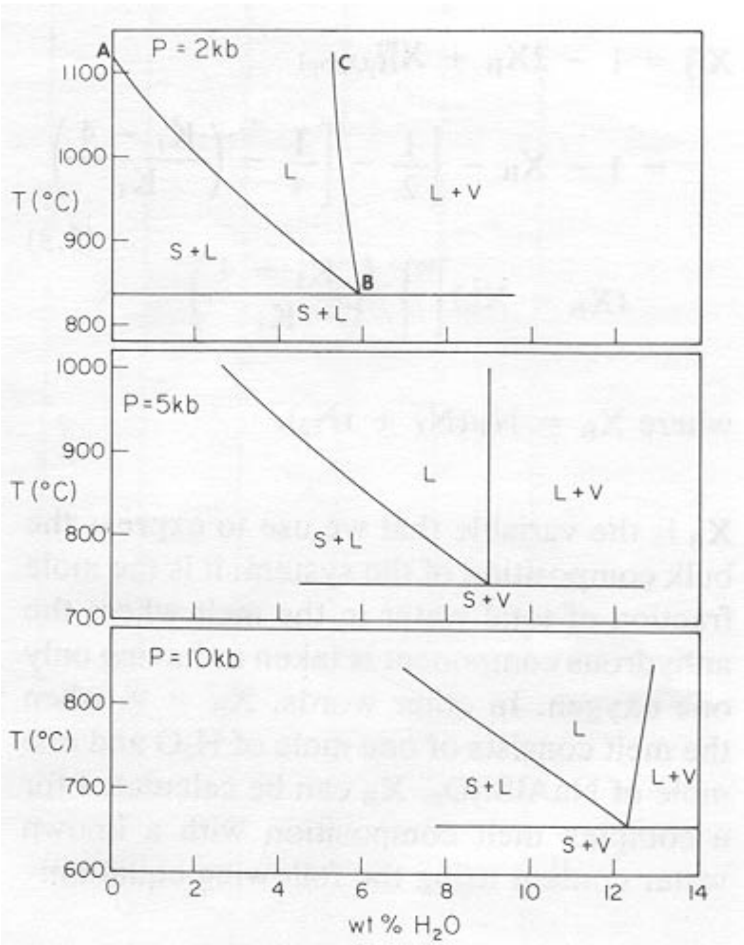

Silver and Stolper (1985) speciation model for melting in simple two component systems mineral – H_2O

Includes molecular H_2O – OH speciation and leads to a planar T – P – X_{H2O} solid – melt boundary

Note linearity of liquidus boundary.

This melting behavior is “adjusted” for perid.

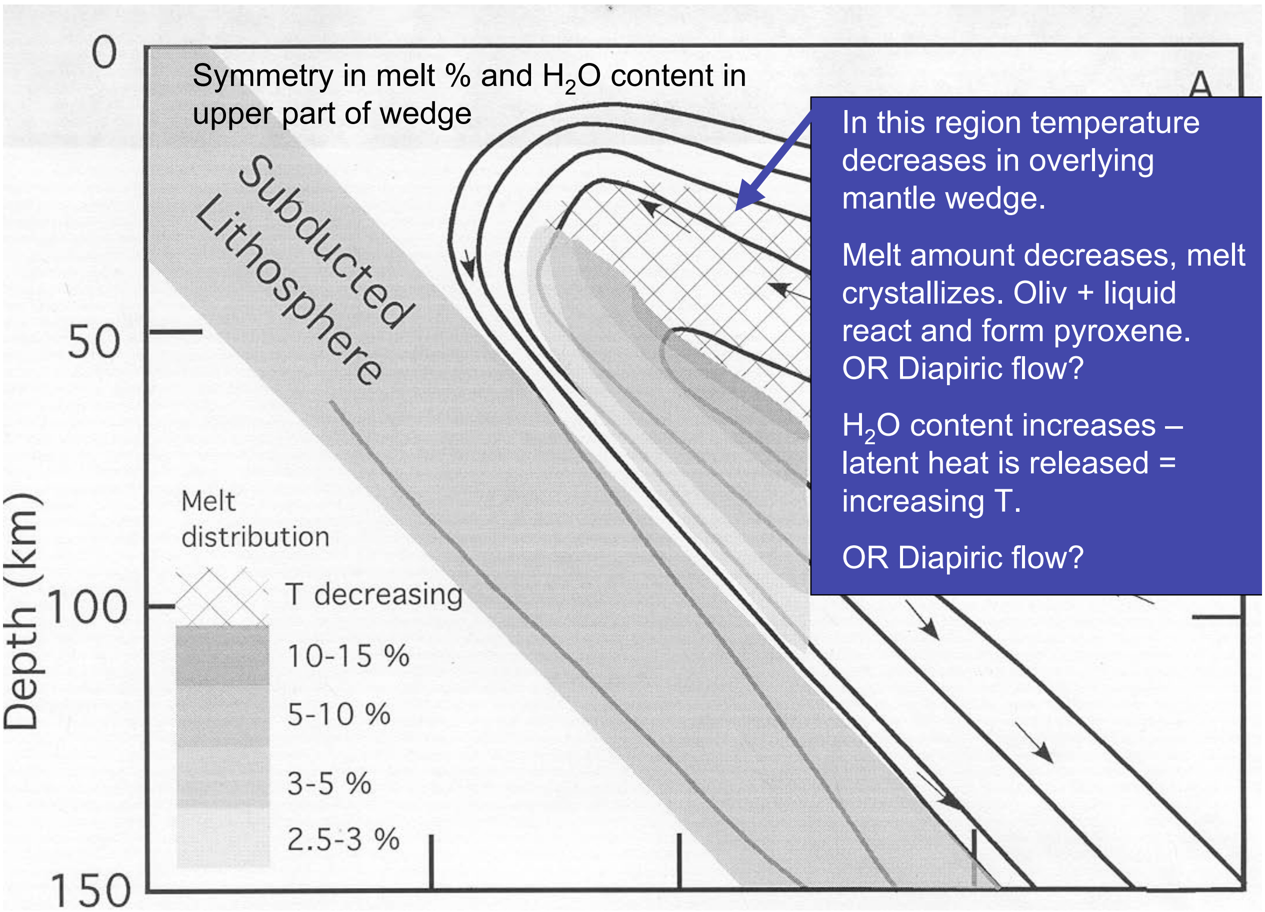

The melting model:

. We use our phase diagram & measured H_2O solubility vs. pressure in forsterite – H_2O to predict the peridotite – melt boundary in T – P – XH_2O space. The expression is:

$$7290*P - 810*T - 24600*H_2O + 1093500 = 0$$

where T is in °C, P is in kilobars and H_2O content is in wt. %.

At P2, T2 the amount of melt ($F_{P2,T2}$) is given by:

$$F_{P2,T2} = ((X_{init} – X_{P2,T2})/X_{init}) * F_{init} + F_{init}$$

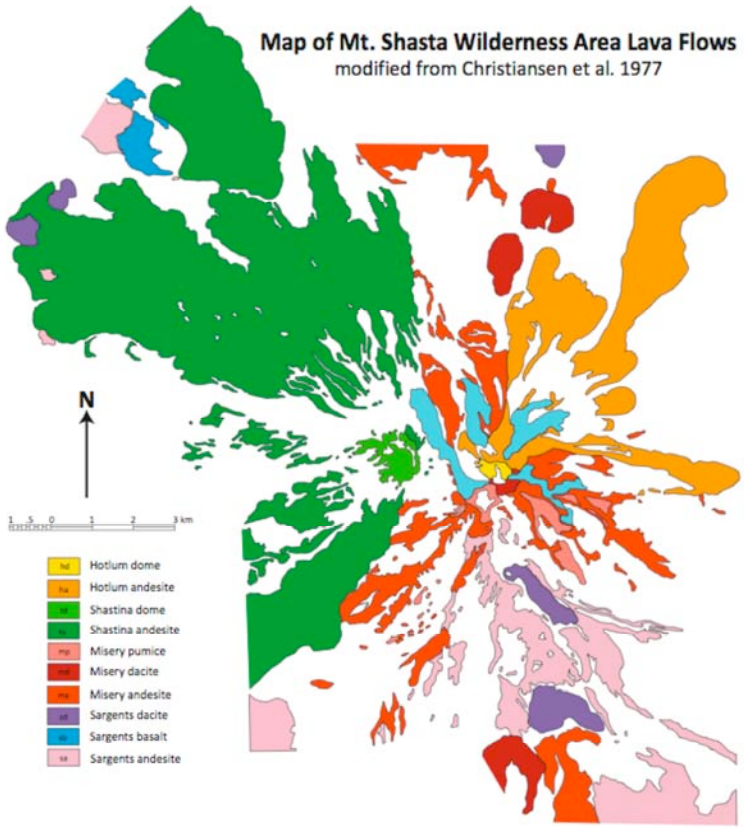

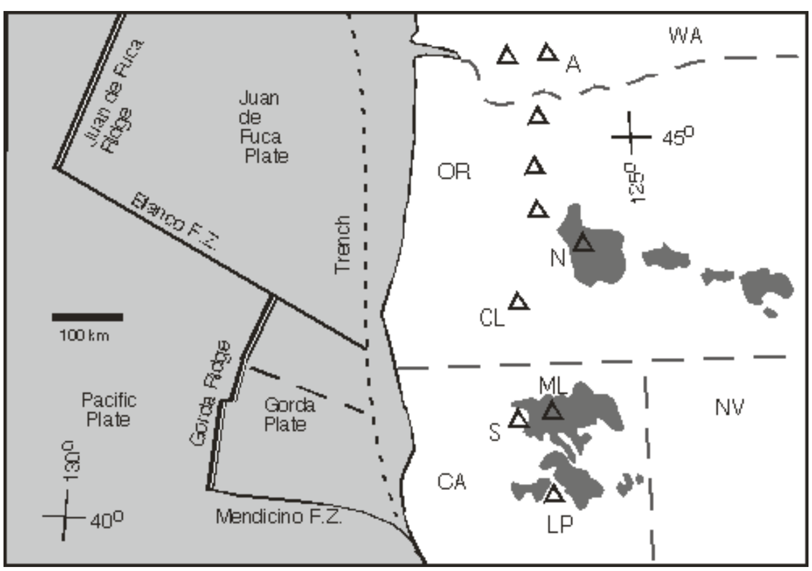

Note the proximity of the Mt. Shasta – Medicine Lake systems to the projection of the Blanco Fracture Zone on the Juan de Fuca plate beneath western edge of North America.


Newberry volcano, Oregon, Big Obsidian Flow and West Paulina Lake
Jay
TLG
Christy
Mike
Etienne

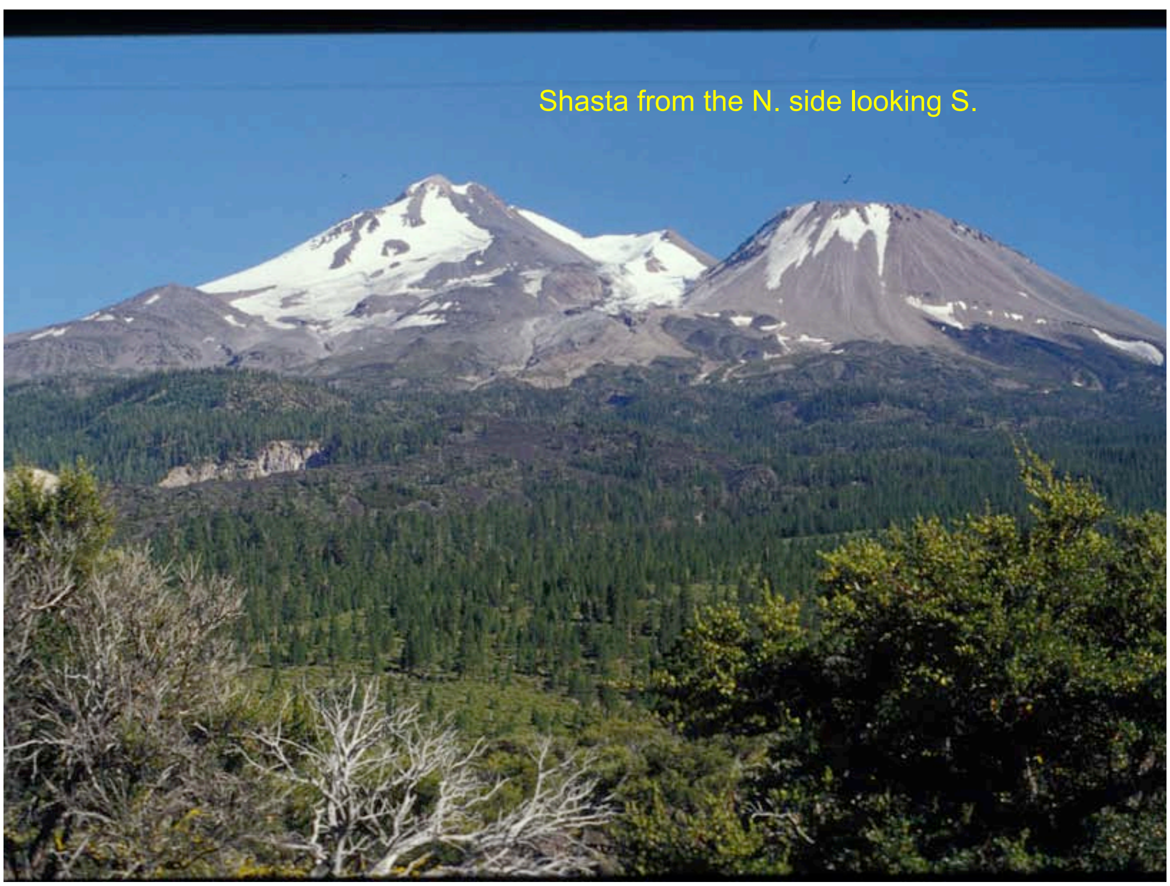
Shasta from the N. side looking S.

Mt. Shasta on the S. side looking N. toward the summit.

Climbing Shasta from the S. side. At the Red Banks.

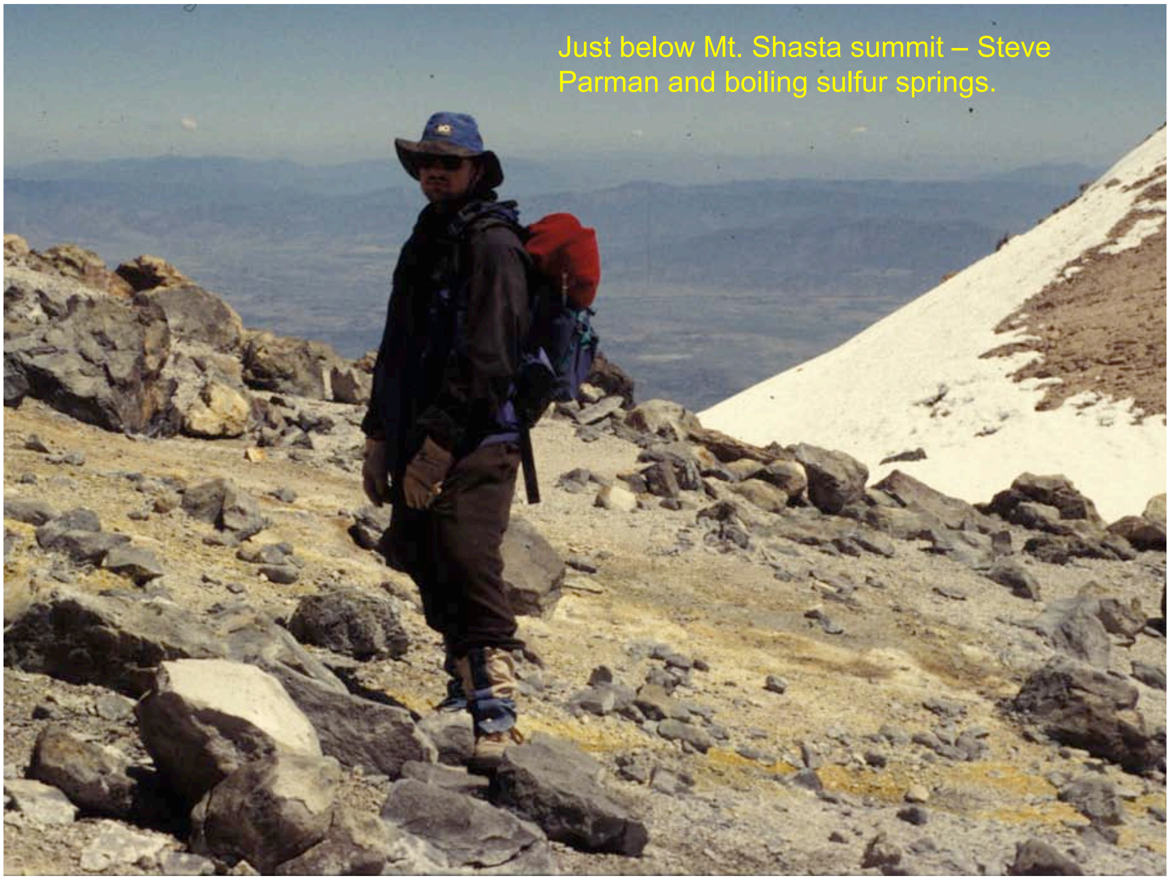

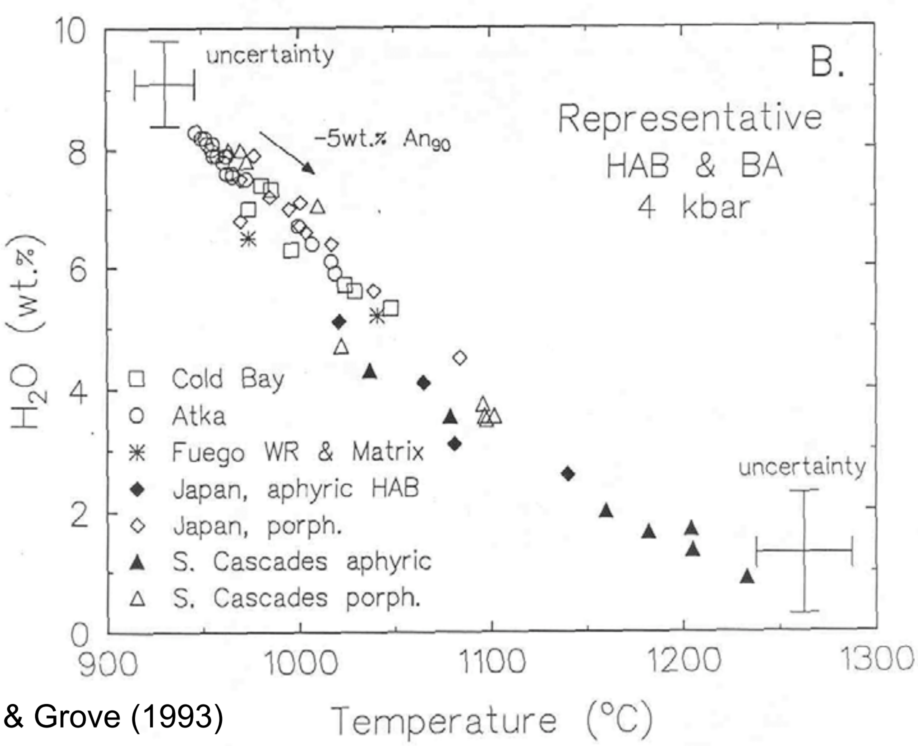

Sisson & Grove (1993)

Estimation of pre-eruptive H_2O content

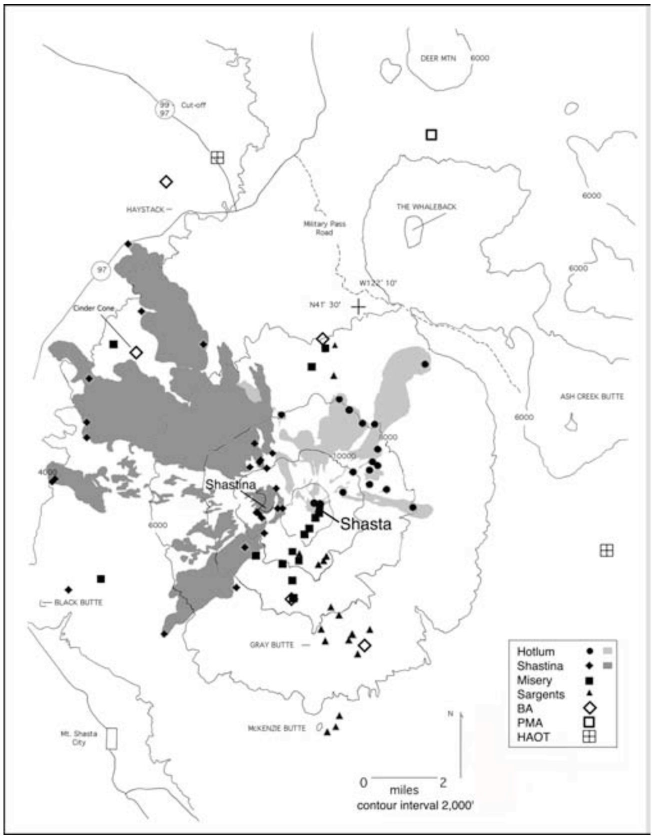

Sampling of Mt. Shasta stratocone and surrounding volcanic vents

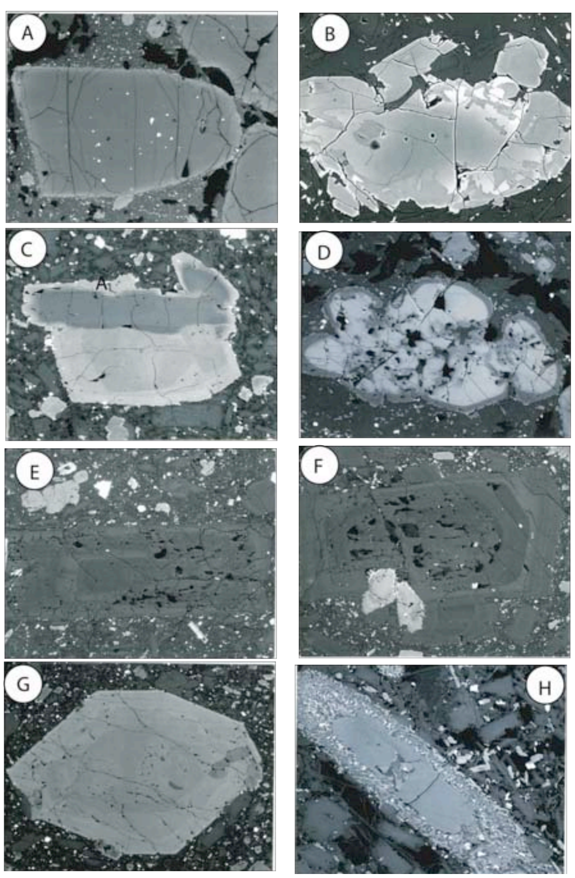

Minerals in Shasta mixed andesite and dacite lavas

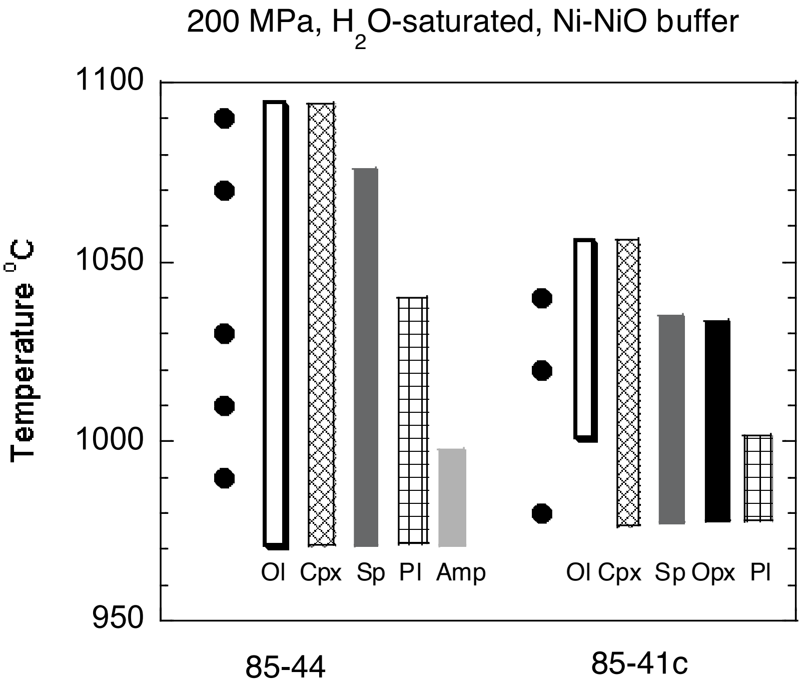

85-44 =
Basaltic
Andesite
53 % SiO_2
10 % MgO
Fo_{90}

85-41 =
Primitive
Magnesian
Andesite
58 % SiO_2
9 % MgO
$Fo_{93.6}$

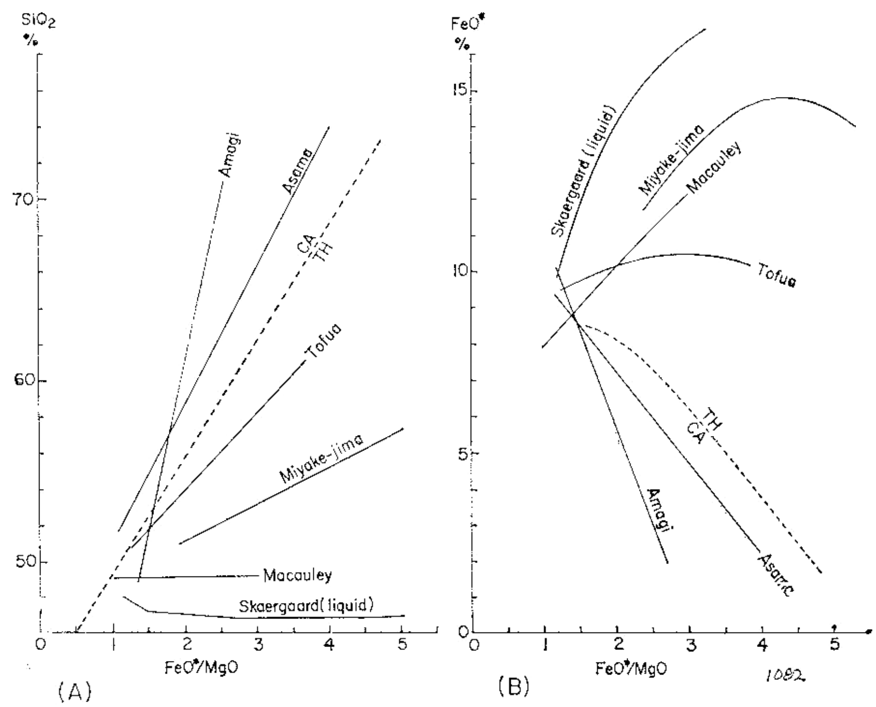

Miyashiro (1974) established the existence of multiple types of liquid lines of descent in sub-alkaline rock series and that these were found in distinct tectonic settings.

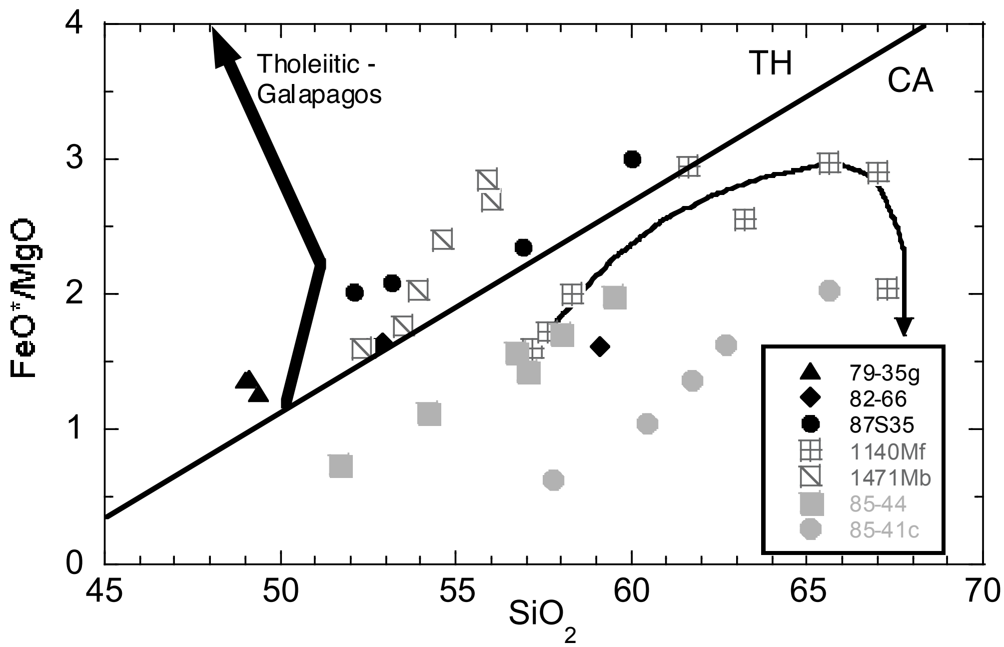

Here are crustal level liquid lines of descent defined by experiments. Galapagos trend is the so-called iron-enrichment trend from Juster et al. (1989). H_2O-bearing experiments are from Sisson and Grove (1993), Medicine Lake and Mt. Shasta experiments discussed on previous days.

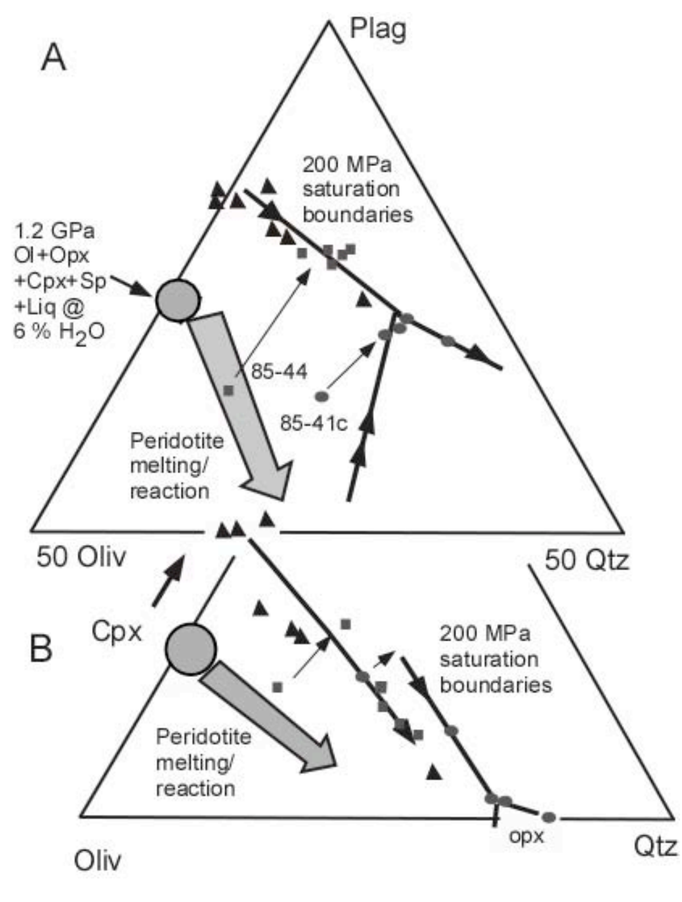

The oliv+opx melting reaction followed during
hydrous mantle melting after cpx + sp are exhausted is shown by
The gray arrow and defines the trend of increasing degree of mantle melting.

Circle shows compositon of hydrous mantle melts from Gaetani & Grove (1998).

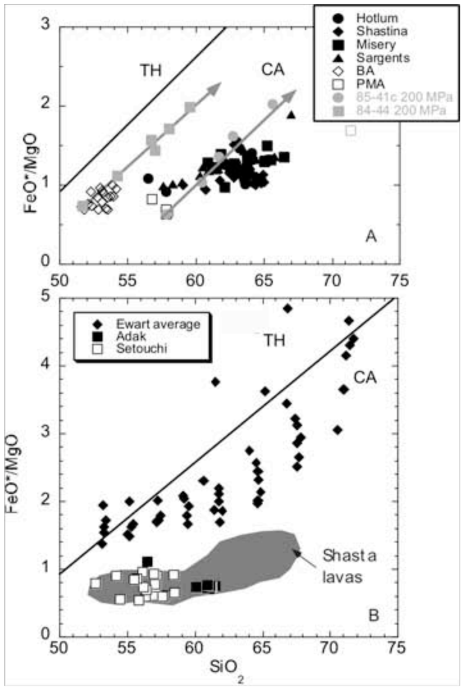

Mt. Shasta andesites, dacites and primitive satellite cone lavas along with experimentally determined liquid lines of descent at 200 MPa and NNO buffer.

Mt. Shasta lavas compared with Ewart's average orogenic andesite averages.

Fig. 1

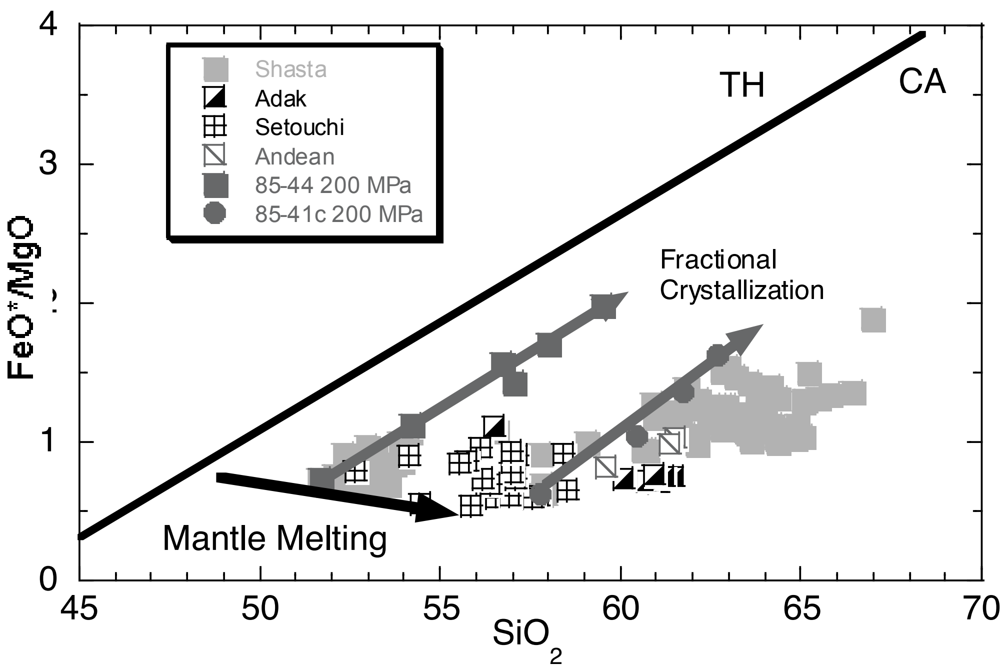

Here we compare the distinct suites of lavas at Setouchi and Adak with the Mt. Shasta lavas and hydrous experimental liquids lines of descent.

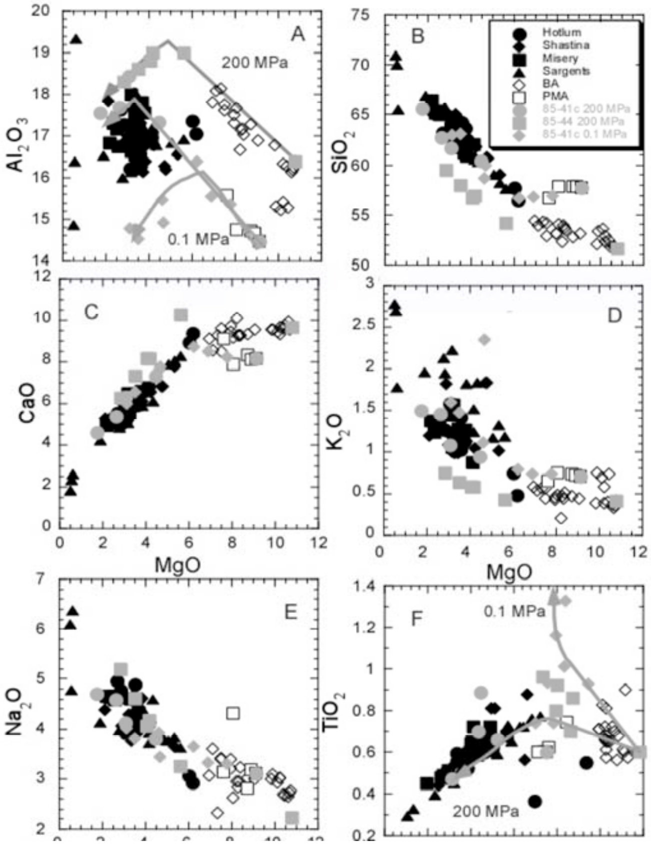

Major element compositional variations in Mt. Shasta region lavas.

Also shown are compositions of BA and PMA lavas and experimentally determined liquid lines of descent from 200 MPa, NNO buffered, H_2O-saturated crystallization experiments on 85-44 and 85-41c

and 0.1 MPa QFM-buffered anhydrous experiments on 85-41c

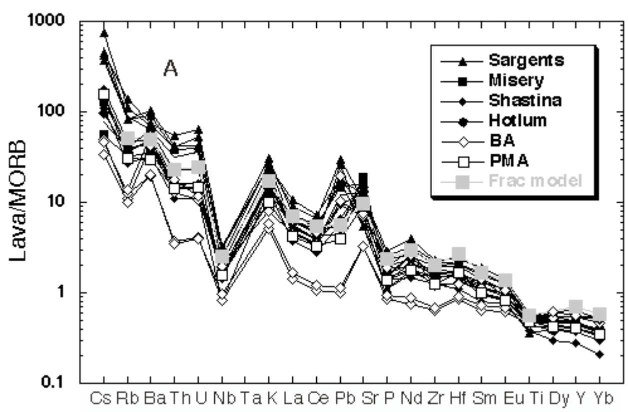

Spidergrams for Mt. Shasta lavas and a comparison of a calculated fractional crystallization model from a primitive magnesian andesite (PMA) parent.

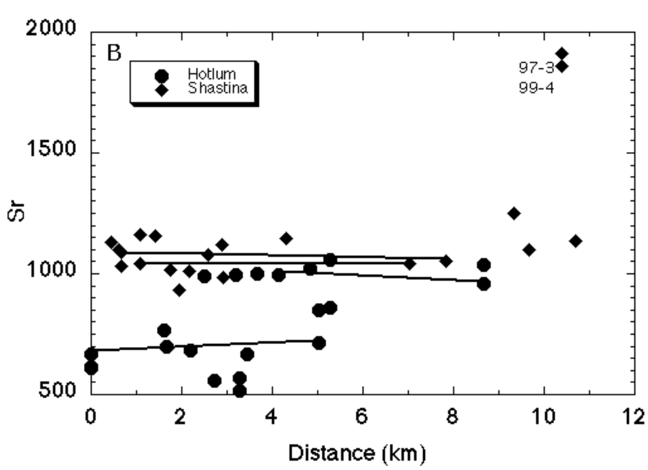

Absense of compositional zoning in Mt. Shasta andesite lava flows. Mixing is very efficient.

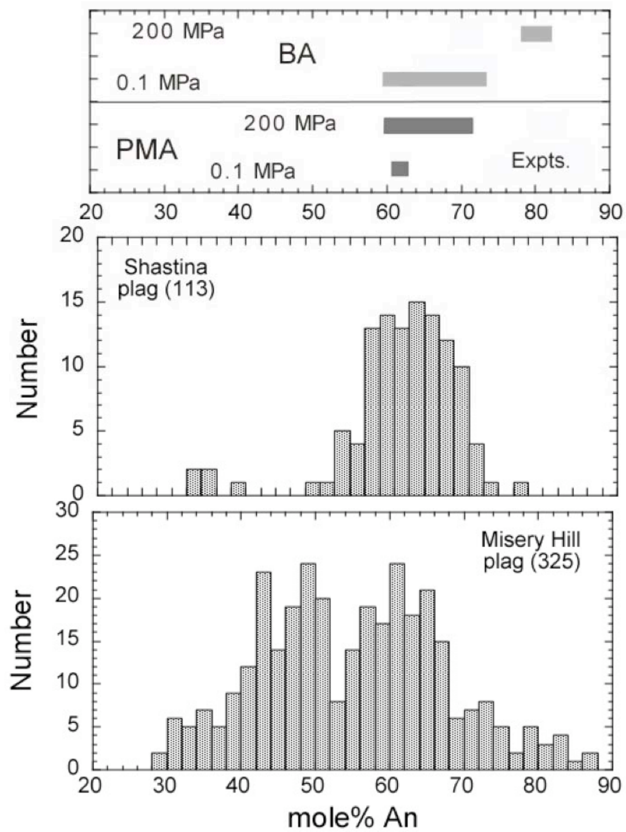

Compositional range of plagioclase produced in 200 MPa, H_2O-saturated and 0.1 MPa anhydrous crystallization experiments on primitive magnesian andesite (PMA) 85-41c and basaltic andesite (BA) 85-44.

Variation in plagioclase phenocryst core compositions of andesites and dacites from the Shastina and Misery eruptive stages.

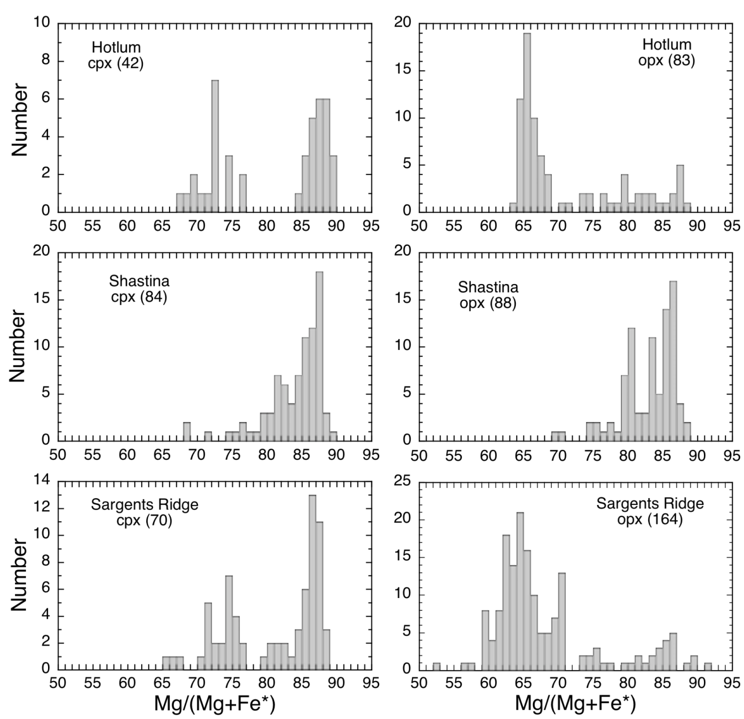

Pyroxene core compositions in Mt. Shasta andesites and dacites.

Horizontal axis: (Mg# = 100*Mg/(Mg+Fe*)).

Each eruptive stage contains preserved evidence for mixing of two or more batches of magma that are at different stages in compositional evolution.

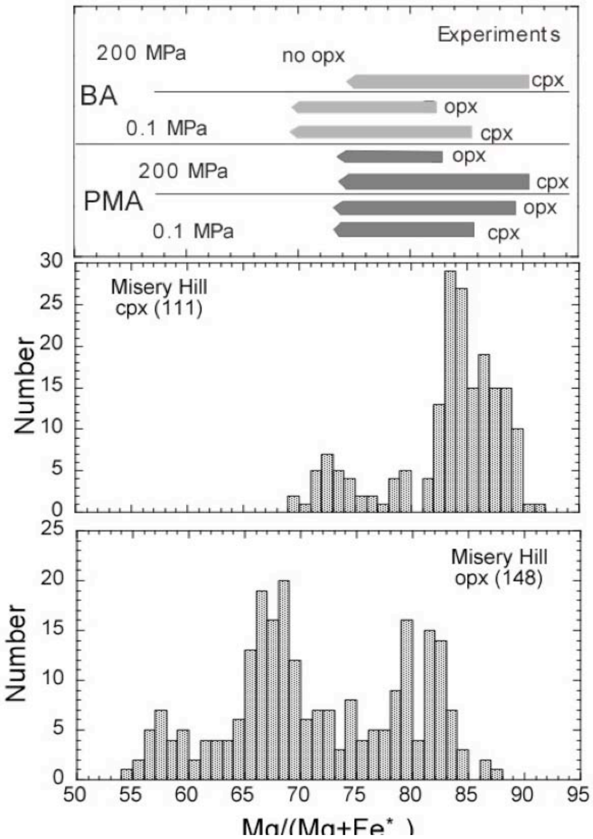

Compositional range of orthopyroxene and augite produced in 200 MPa, H_2O-saturated and 0.1 MPa anhydrous crystallization experiments on basaltic andesite (BA) 85-44 and primitive magnesian andesite (PMA) 85-41c.

Variation in phenocryst core composition found in orthopyroxene (opx) and augite (cpx) of andesites and dacites from the Misery eruptive stage.

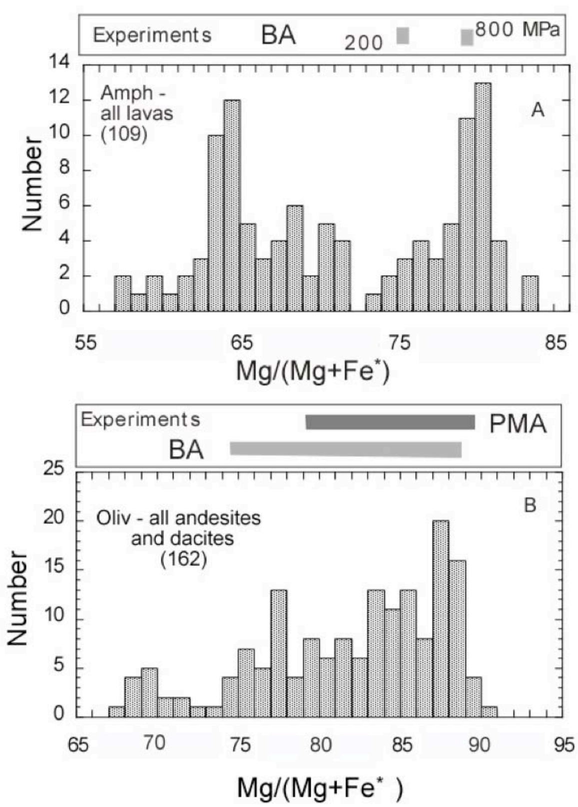

Variation in phenocryst core compositions of amphibole (A) and olivine (B) from all Shasta region andesites and dacites. Horizontal axis is (Mg# = 100*Mg/(Mg+Fe*)).

Numbers in parentheses are the number of analyses used in each histogram.

Experimental amphiboles are from 200 and 800 MPa, H_2O-saturated experiments on 85-44.

Experimental olivine compositions are from 200 MPa runs.

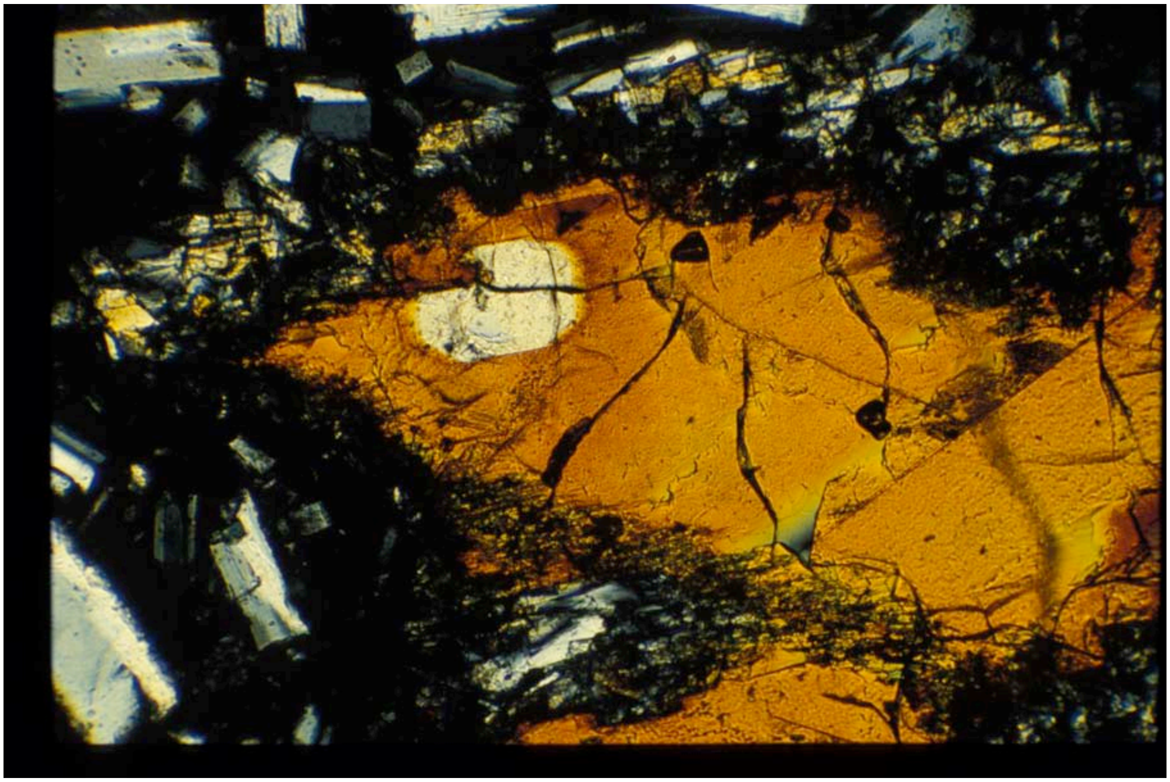

Amphibole in Shastina lava in overgrowth reaction with rthopyroxene. ~ 0.5 mm FOV

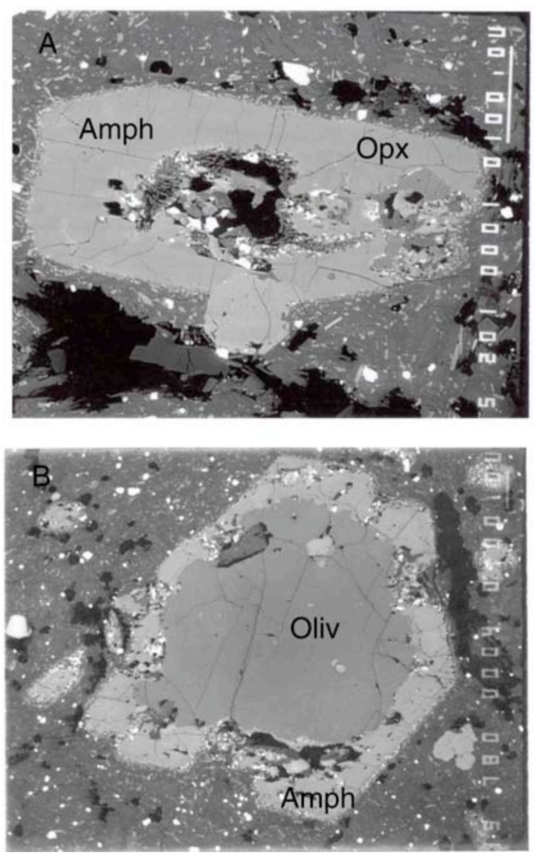

Backscattered images of magnesian amphbole overgrowing Mg-rich pyroxene and olivine in Mt. Shasta andesites.

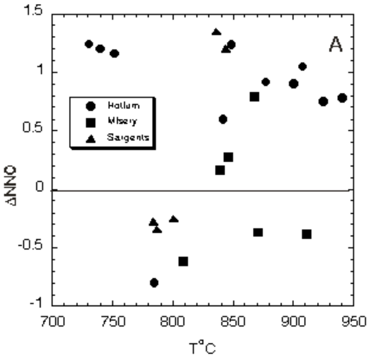

Oxide thermobarometry from magnetite-ulvospinel ss and hematite-ilmenite ss assemblages. Note the range of oxygen fugacities.

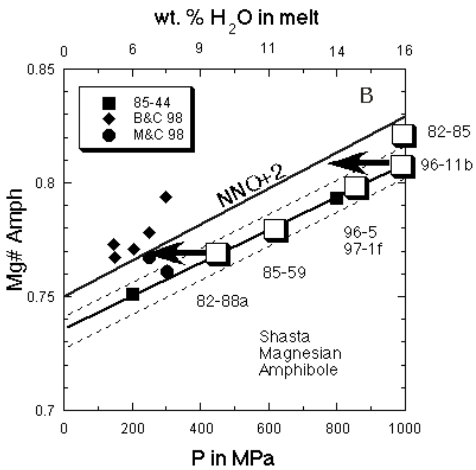

Experimental calibration of pressure and H_2O content of crystallization of amphiboles found in Shasta andesite lavas and quenched magmatic inclusions.

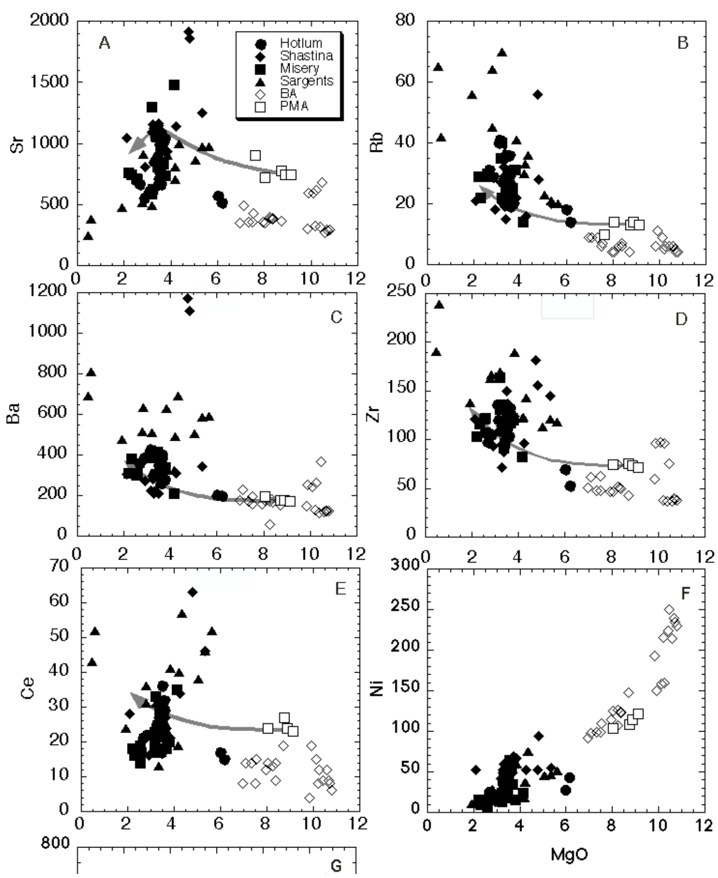

Trace element abundance variations in Mt. Shasta stratocone lavas and a fractional crystallization model.

Model uses phase proportions from 200 MPa crystallization experiments on the primitive magnesian andesite (PMA).

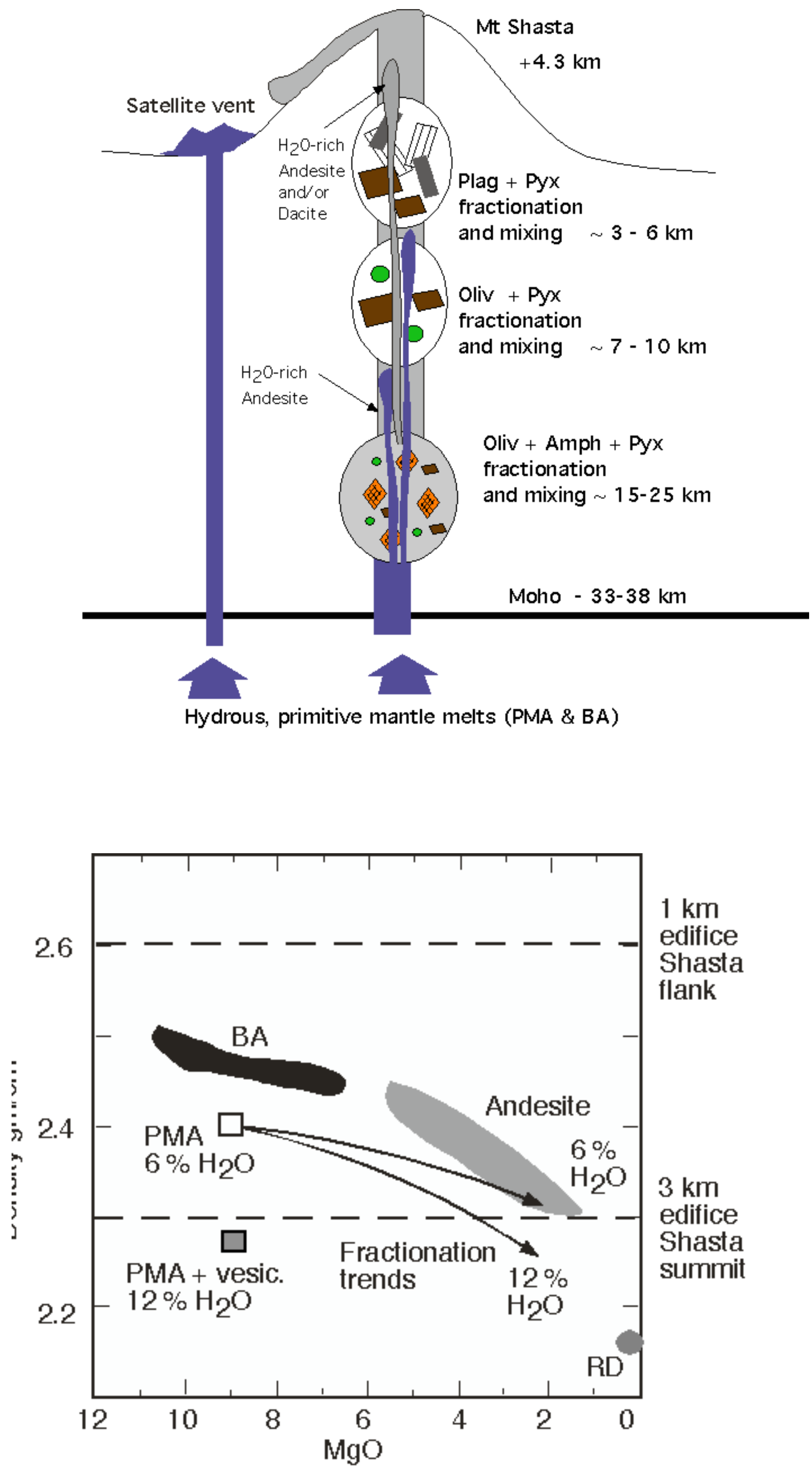

Constraints on magma eruptability beneath the Mt. Shasta edifice.

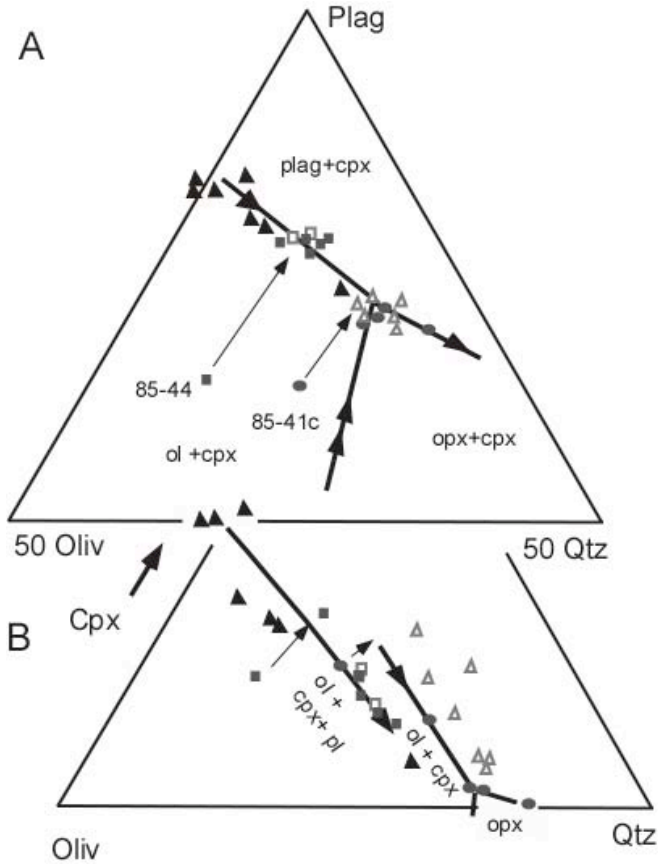

Phase relations at 200 MPA for the primitive lavas at Mt. Shasta.

Projection schemes use oxygen units.

Magma Processing in the Lower Crust As recorded in mafic inclusions from Mt. Shasta, CA

Mike Krawczynski and Tim Grove

- QMI's link primitive flank lavas to evolved andesites
- H_2O saturated experiments spanning crust
- Where is magma processing occurring in the crust?
- Eruptibility of mafic melts in the case of Mt. Shasta

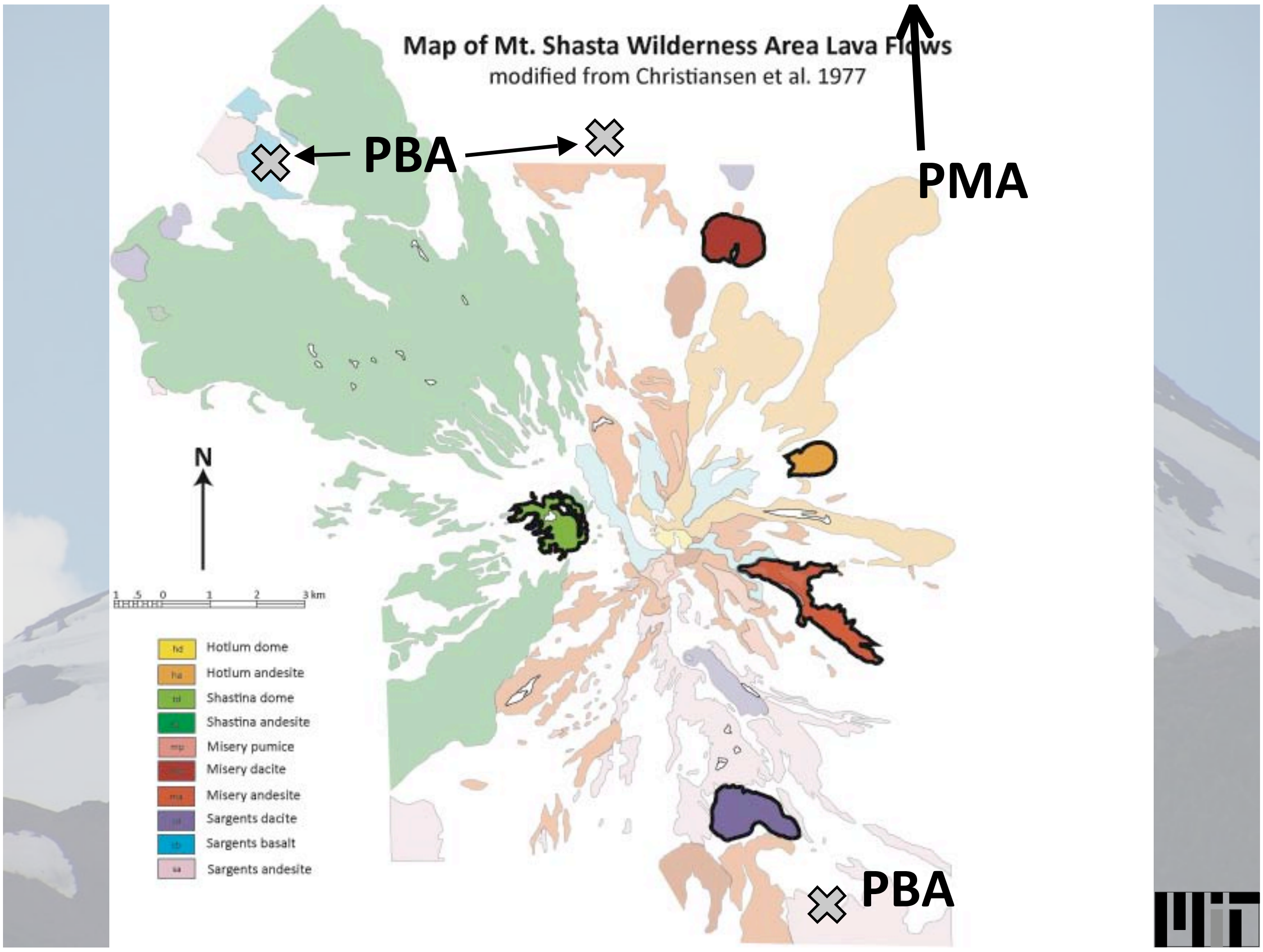
Map of Mt. Shasta Wilderness Area Lava Flows
modified from Christiansen et al. 1977
PBA
PMA
PBA
N
1 .5 0 1 2 3 km
Hotlum dome
Hotlum andesite
Shastina dome
Shastina andesite
Misery pumice
Misery dacite
Misery andesite
Sargents dacite
Sargents basalt
Sargents andesite

A successful inclusion hunt at Mt. Shasta

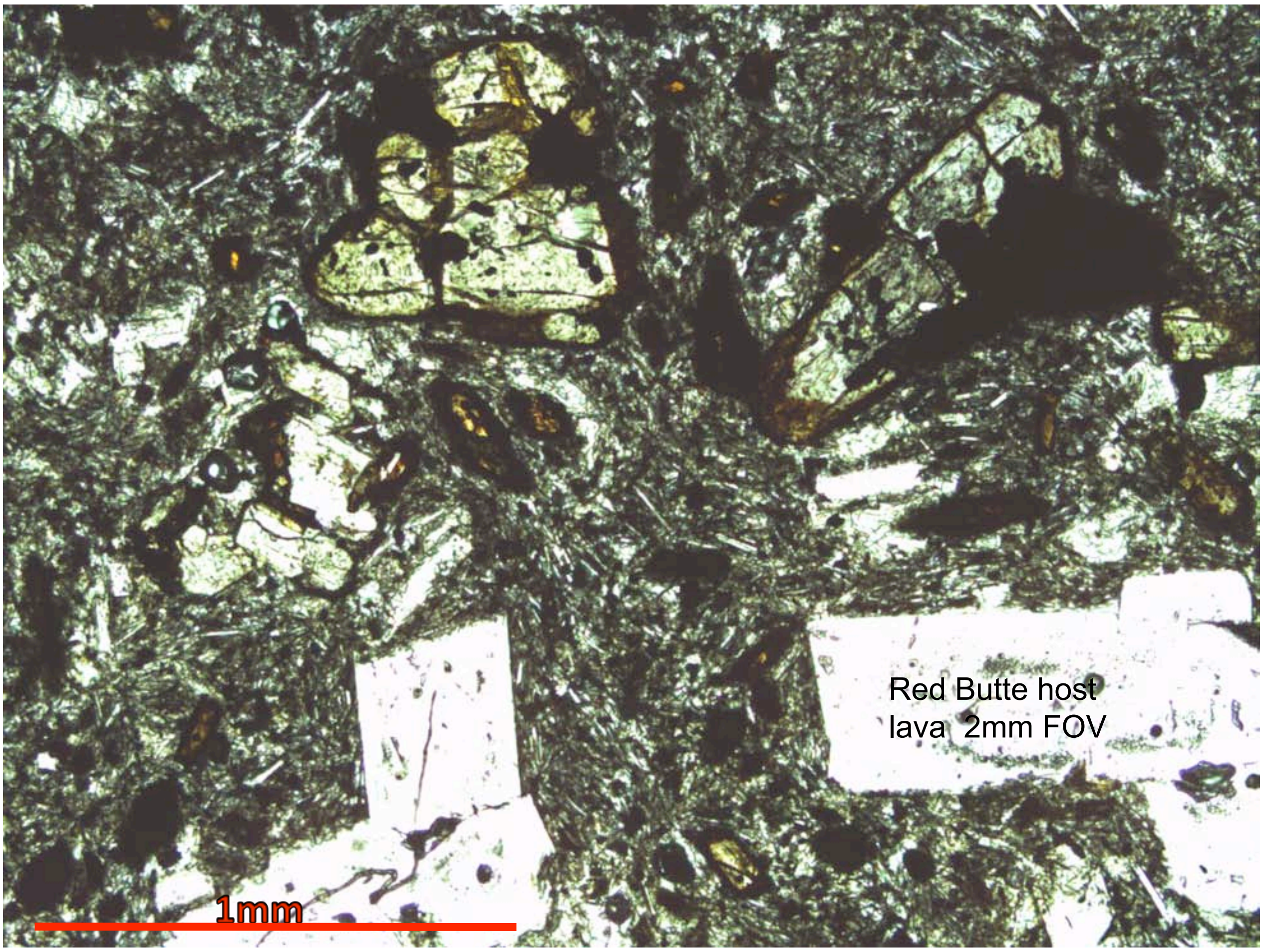

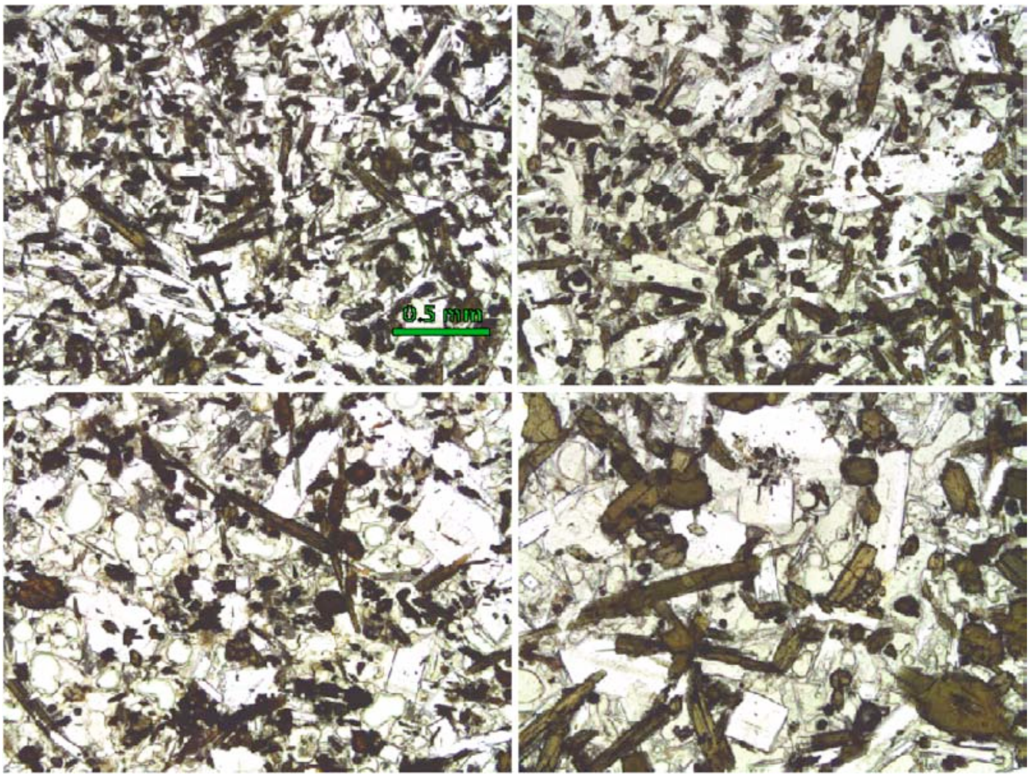

Textural variability in quenched magmatic inclusions in Mt. Shasta lavas

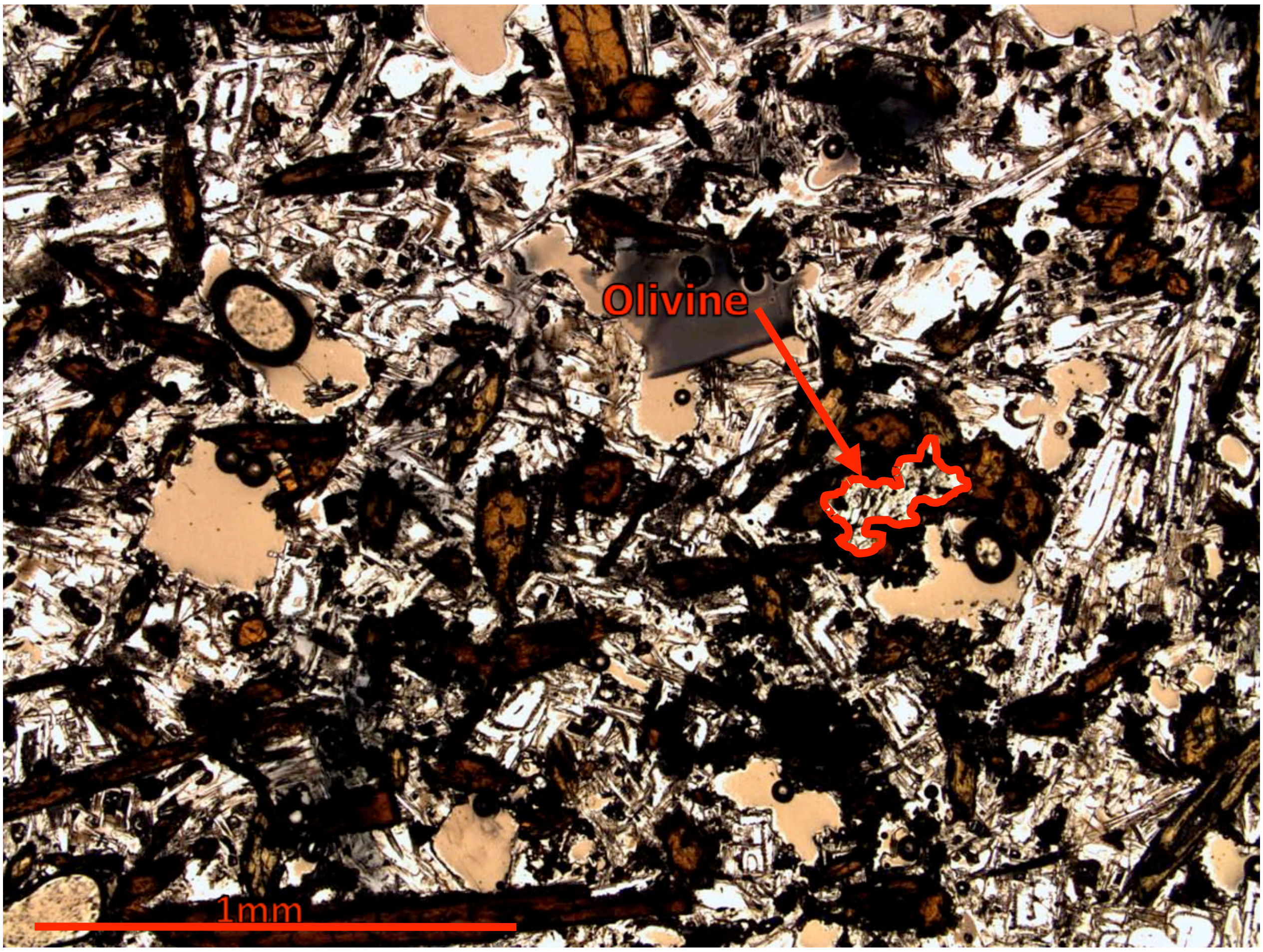
Olivine
1mm

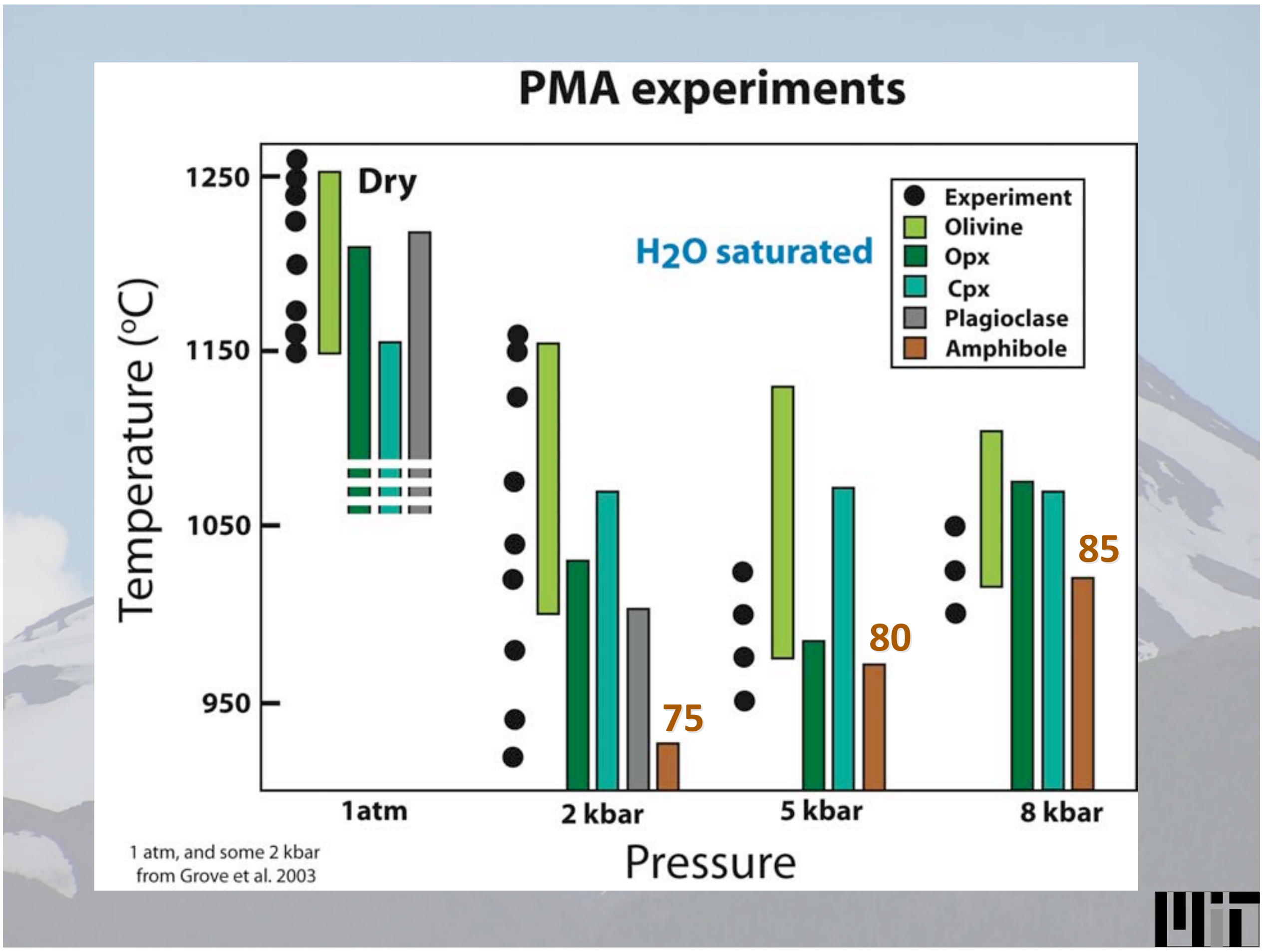
PMA experiments
Dry
H2O saturated
Experiment
Olivine
Opx
Cpx
Plagioclase
Amphibole
1250
1150
1050
950
Temperature (°C)
75
80
85
1atm
2 kbar
5 kbar
8 kbar
Pressure
1 atm, and some 2 kbar
from Grove et al. 2003

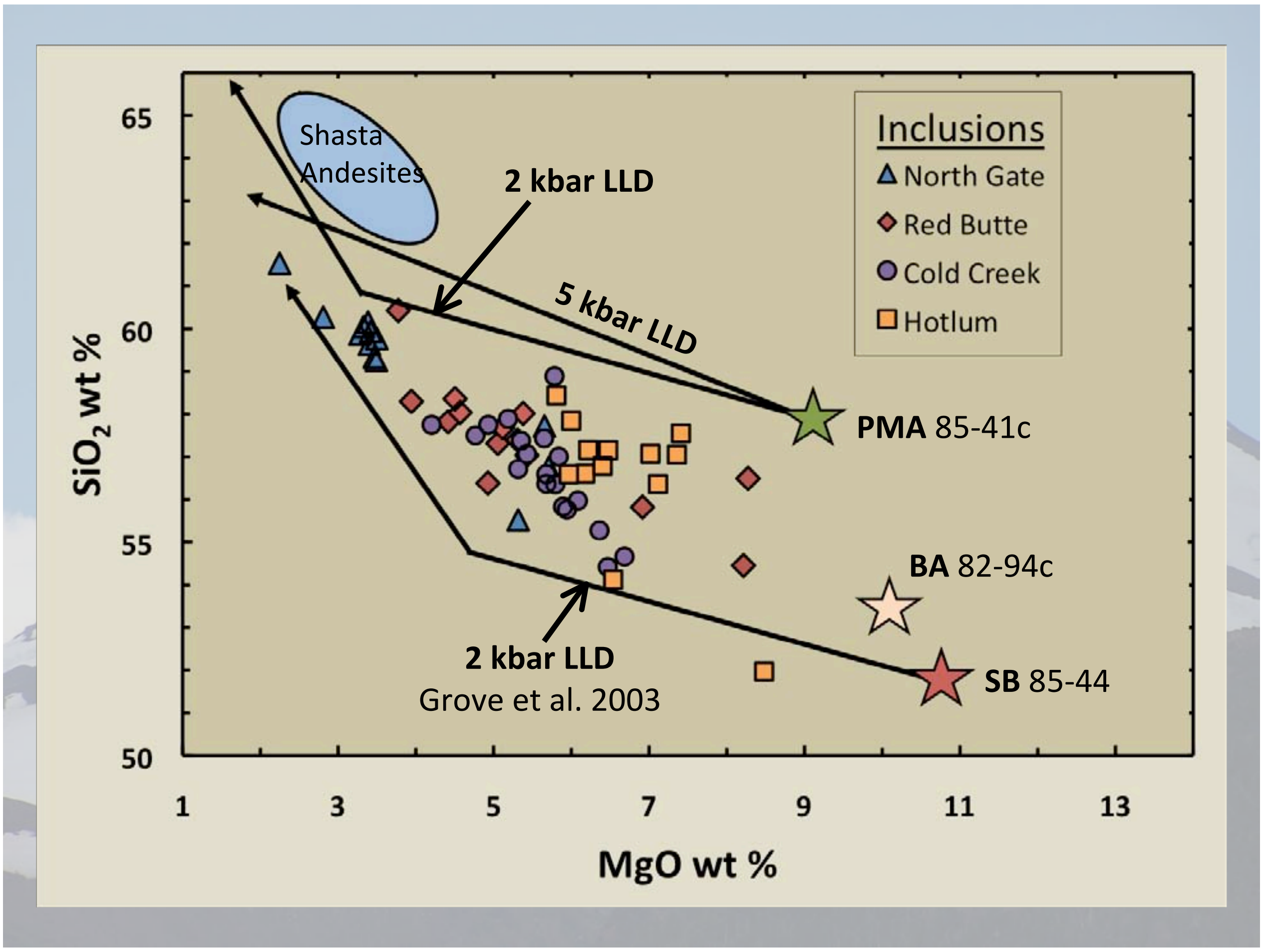

Inclusions
North Gate
Red Butte
Cold Creek
Hotlum
Shasta Andesites
2 kbar LLD
5 kbar LLD
PMA 85-41c
BA 82-94c
SB 85-44
2 kbar LLD
Grove et al. 2003
SiO_2 wt %
MgO wt %
65
60
55
50
1
3
5
7
9
11
13

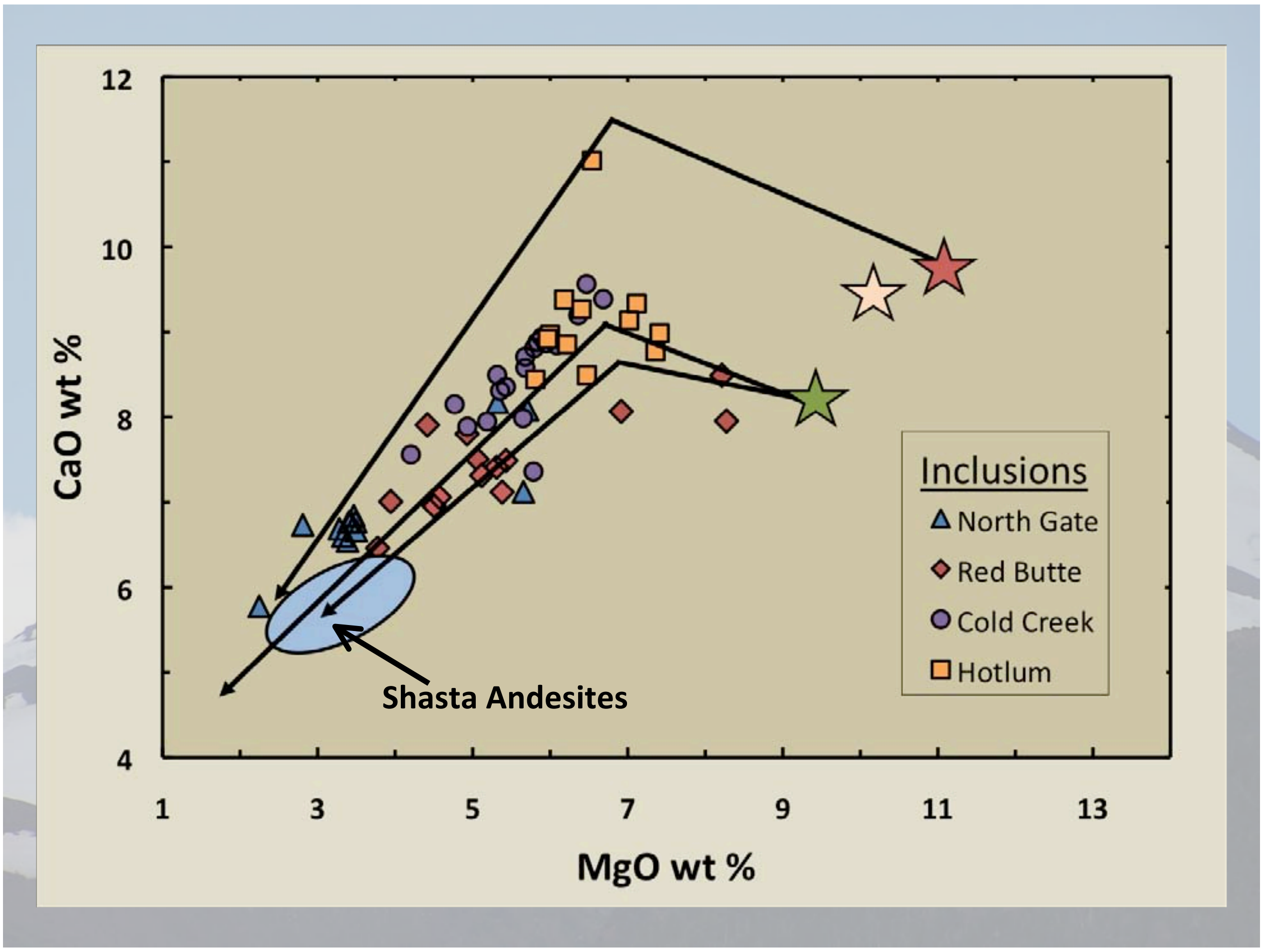

Inclusions
North Gate
Red Butte
Cold Creek
Hotlum
Shasta Andesites
CaO wt %
MgO wt %
12
10
8
6
4
1
3
5
7
9
11
13

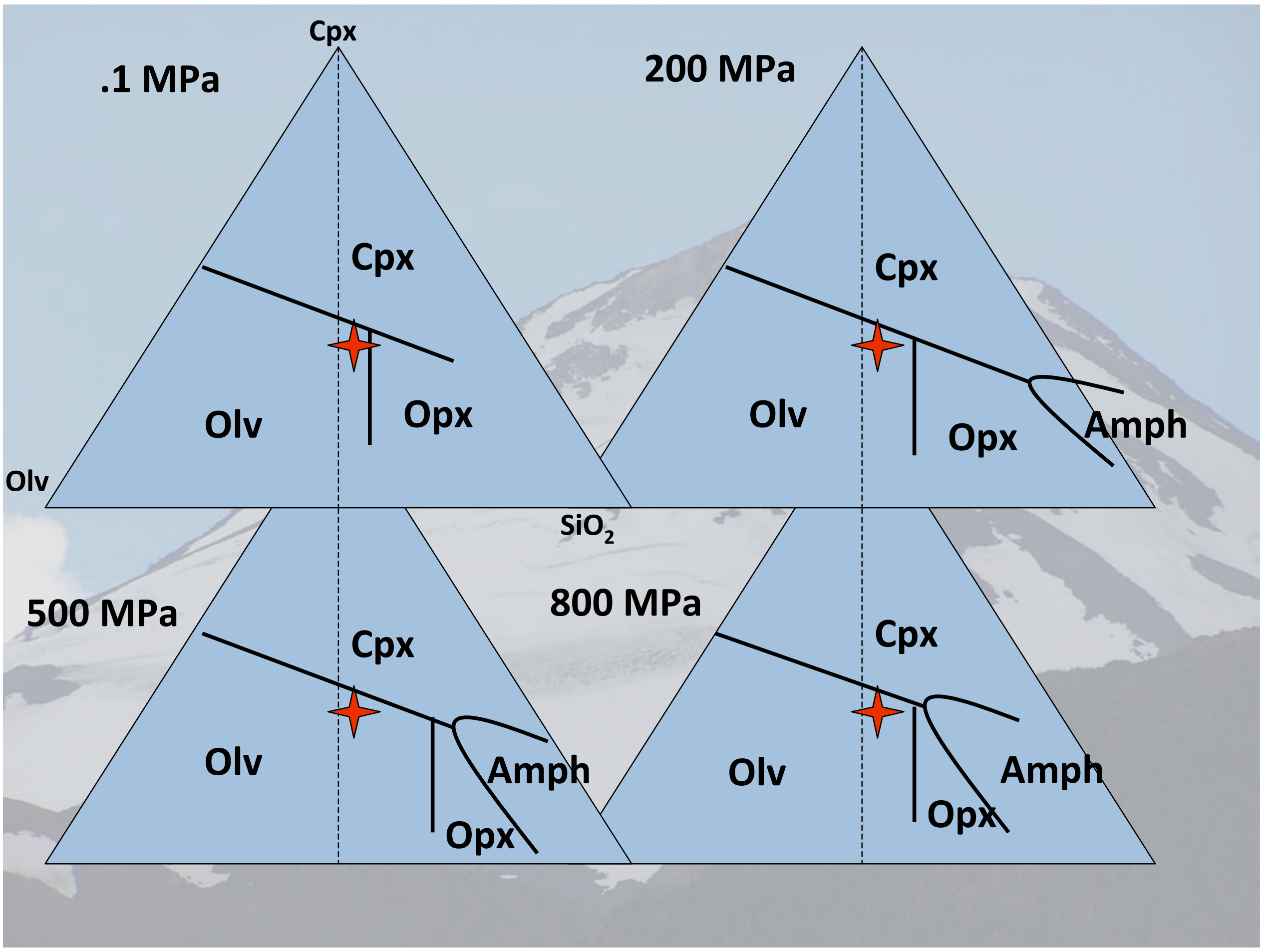

Cpx
.1 MPa
200 MPa
Cpx
Olv
Opx
Olv
Cpx
Olv
Opx
Amph
SiO2
500 MPa
Cpx
Olv
Amph
Opx
800 MPa
Cpx
Olv
Amph
Opx

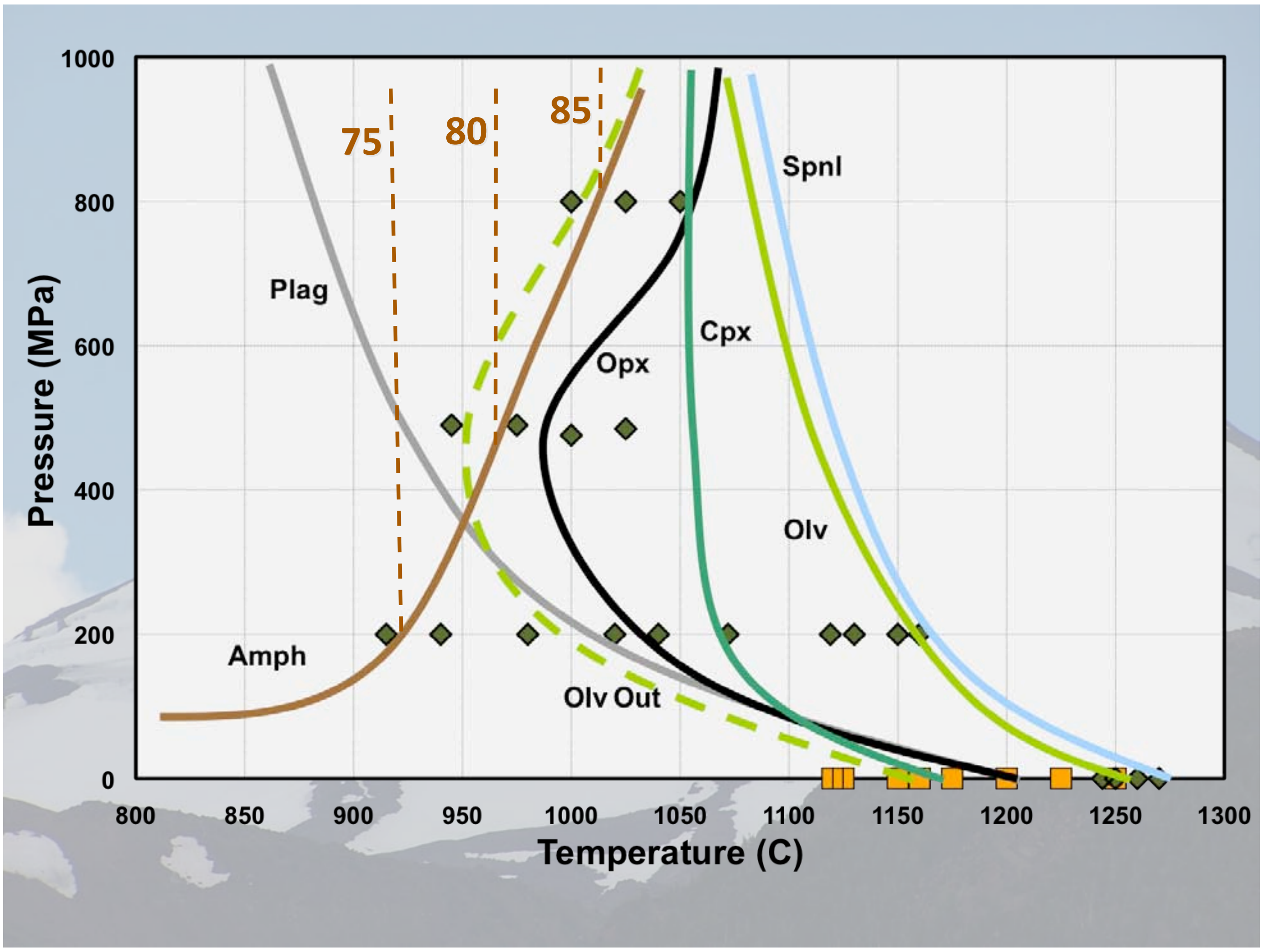

Pressure (MPa)
1000
800
600
400
200
0
75
80
85
Spnl
Plag
Cpx
Opx
Olv
Amph
Olv Out
800
850
900
950
1000
1050
1100
1150
1200
1250
1300
Temperature (C)

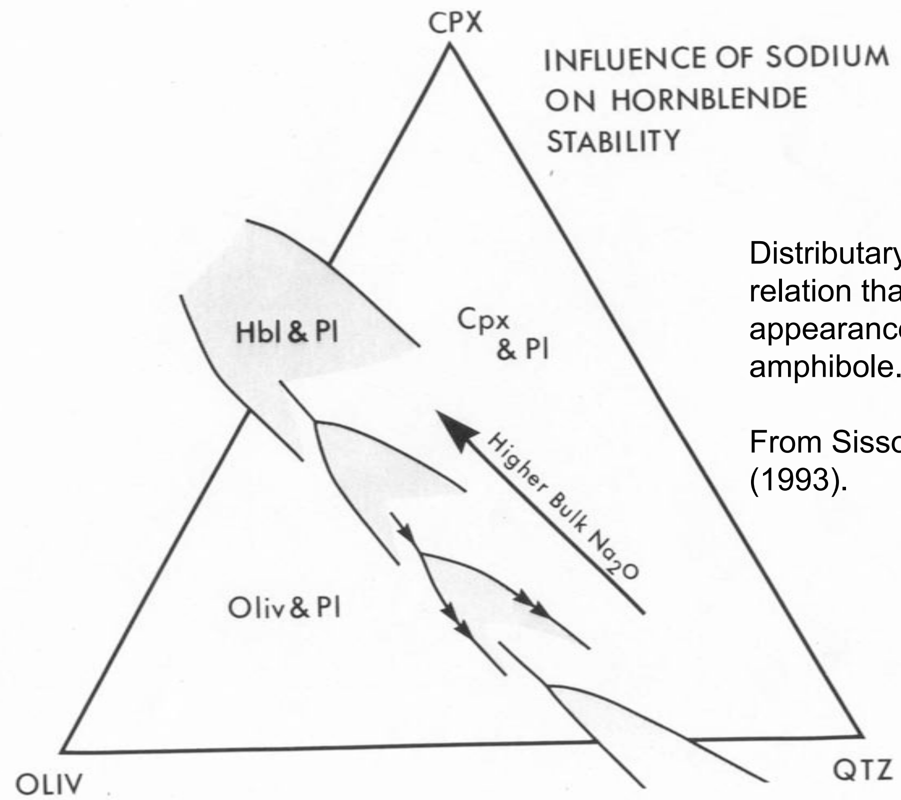

Distributary reaction relation that leads to the appearance of amphibole.

From Sisson and Grove (1993).

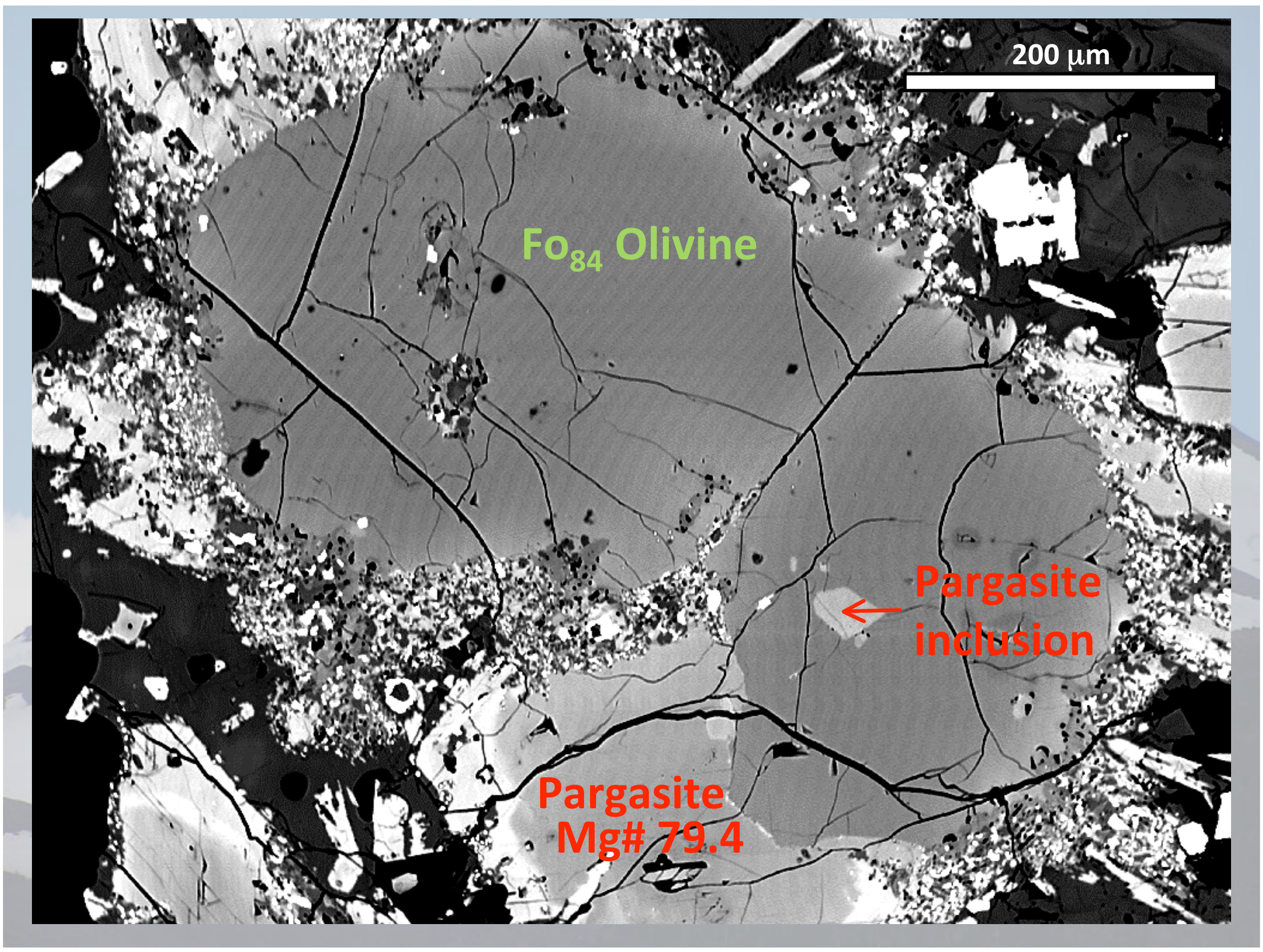

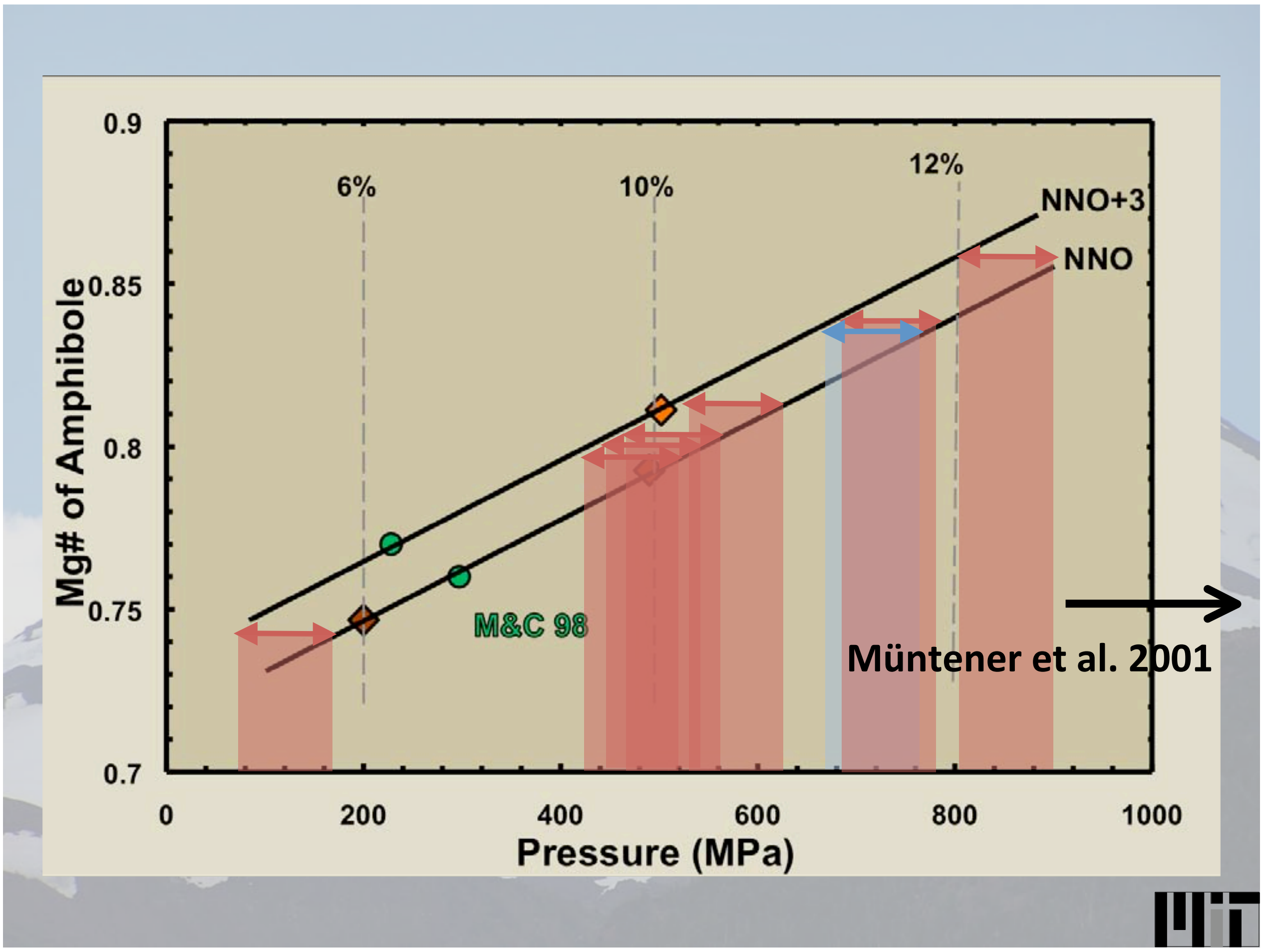

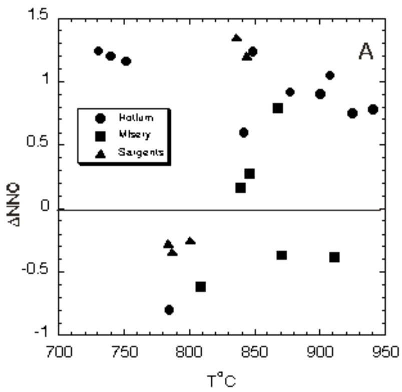

Oxide thermobarometry from magnetite-ulvospinel ss and hematite-ilmenite ss assemblages. Note the range of oxygen fugacities.

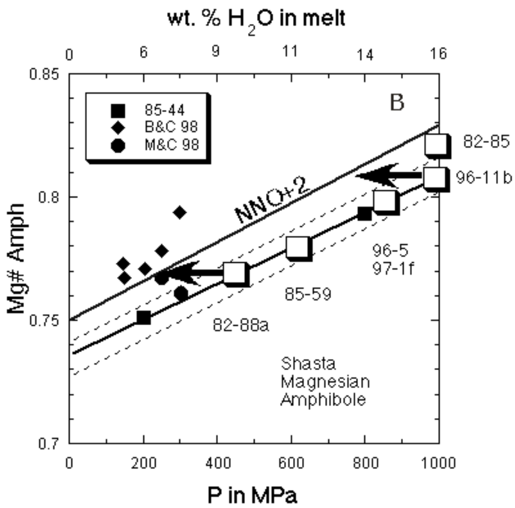

Experimental calibration of pressure and H_2O content of crystallization of amphiboles found in Shasta andesite lavas and quenched magmatic inclusions.

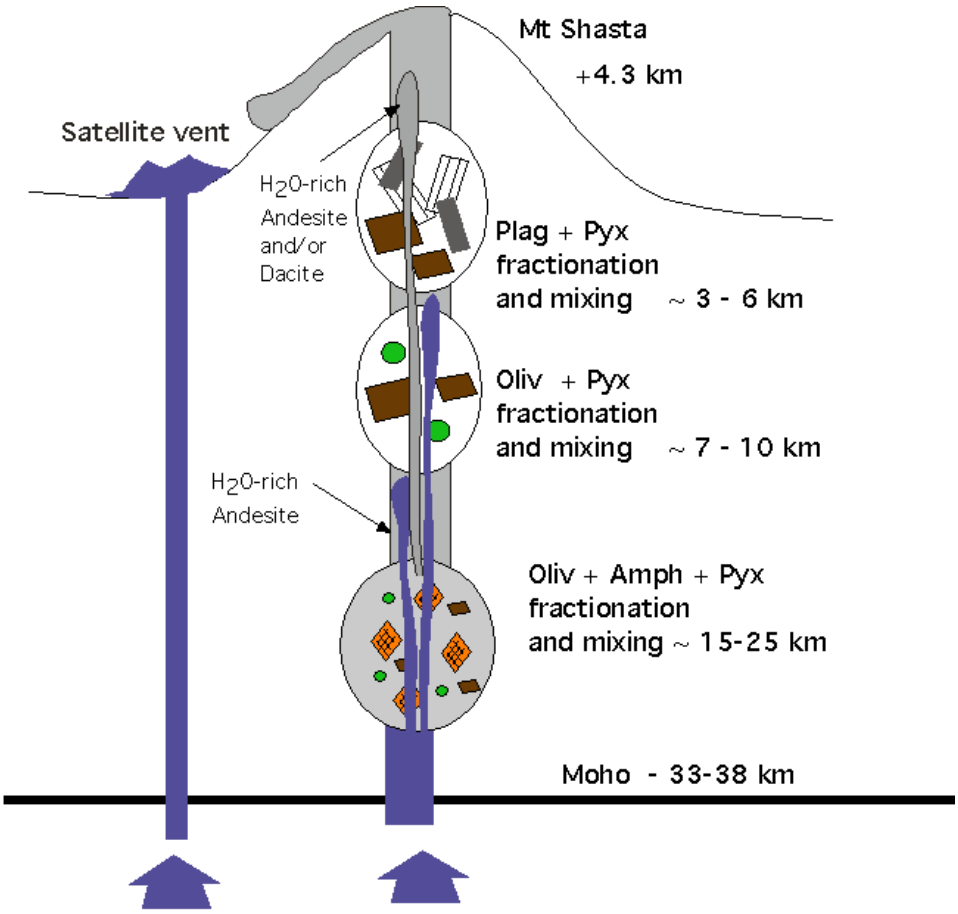

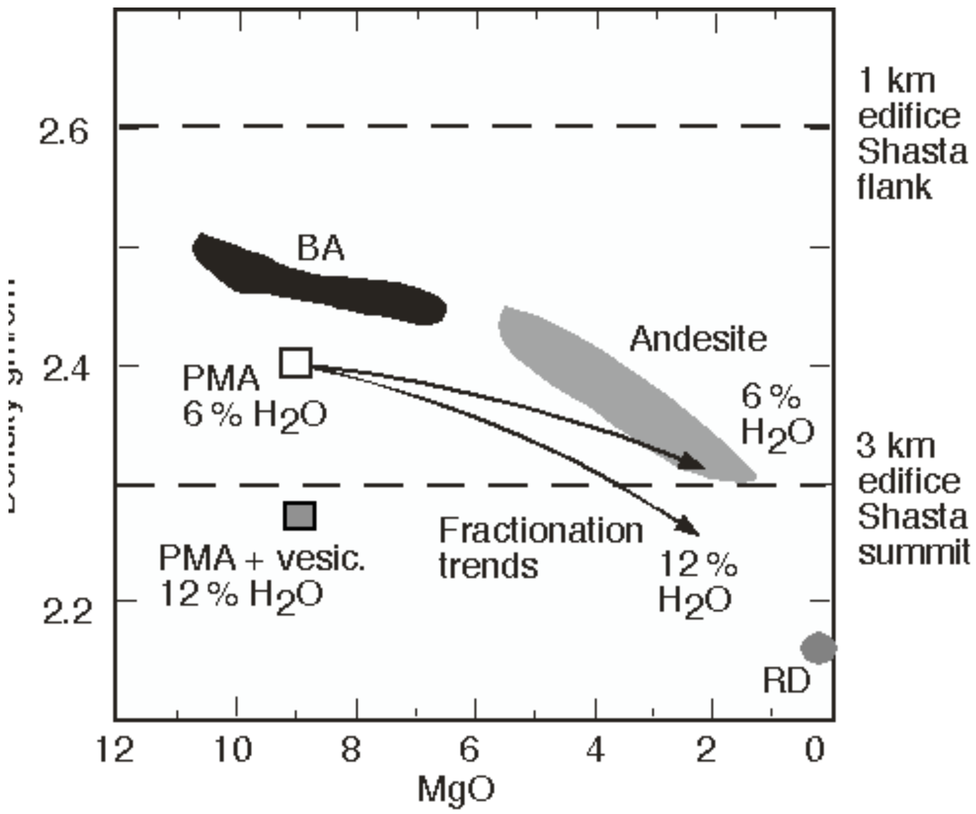

Constraints on magma eruptability beneath the Mt. Shasta edifice.

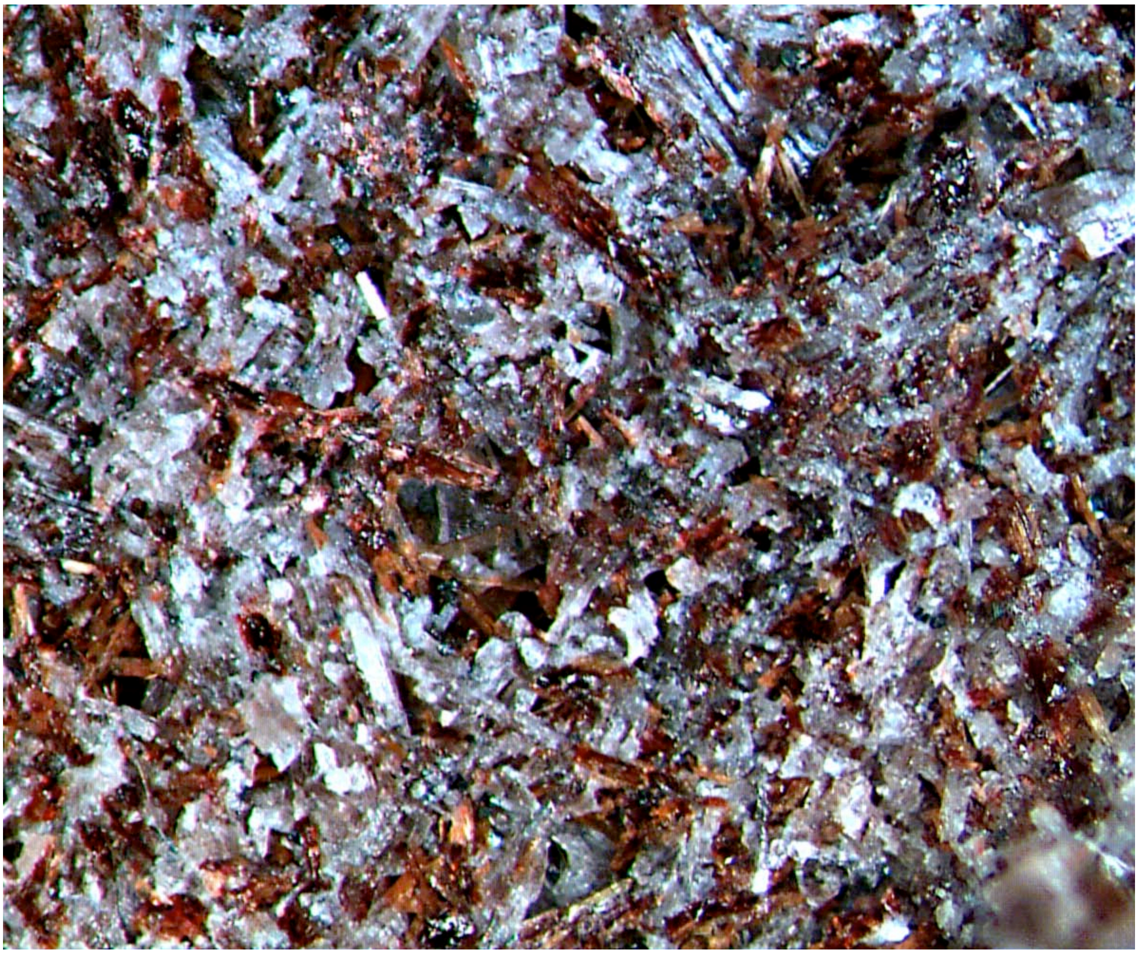

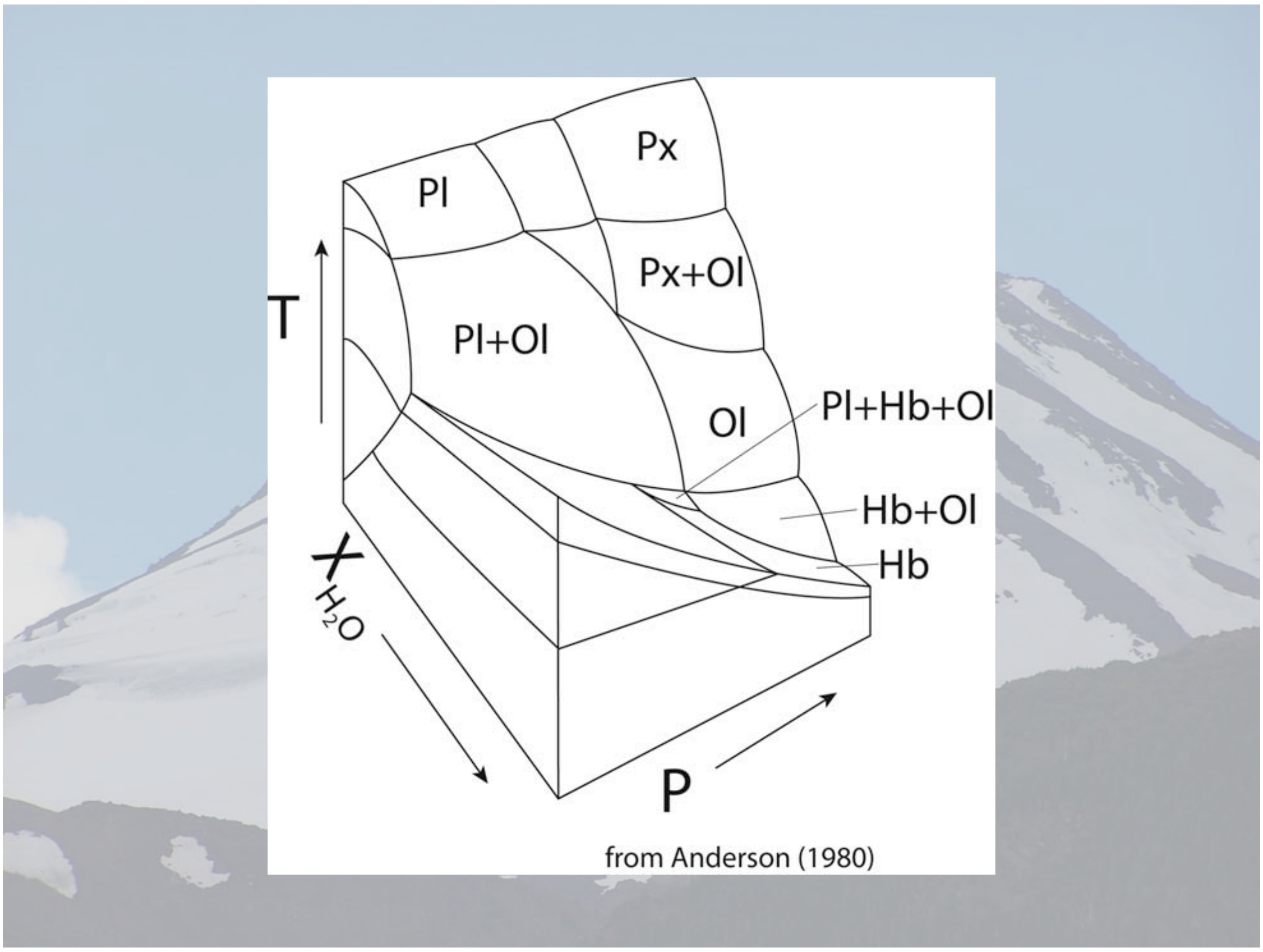

from Anderson (1980)

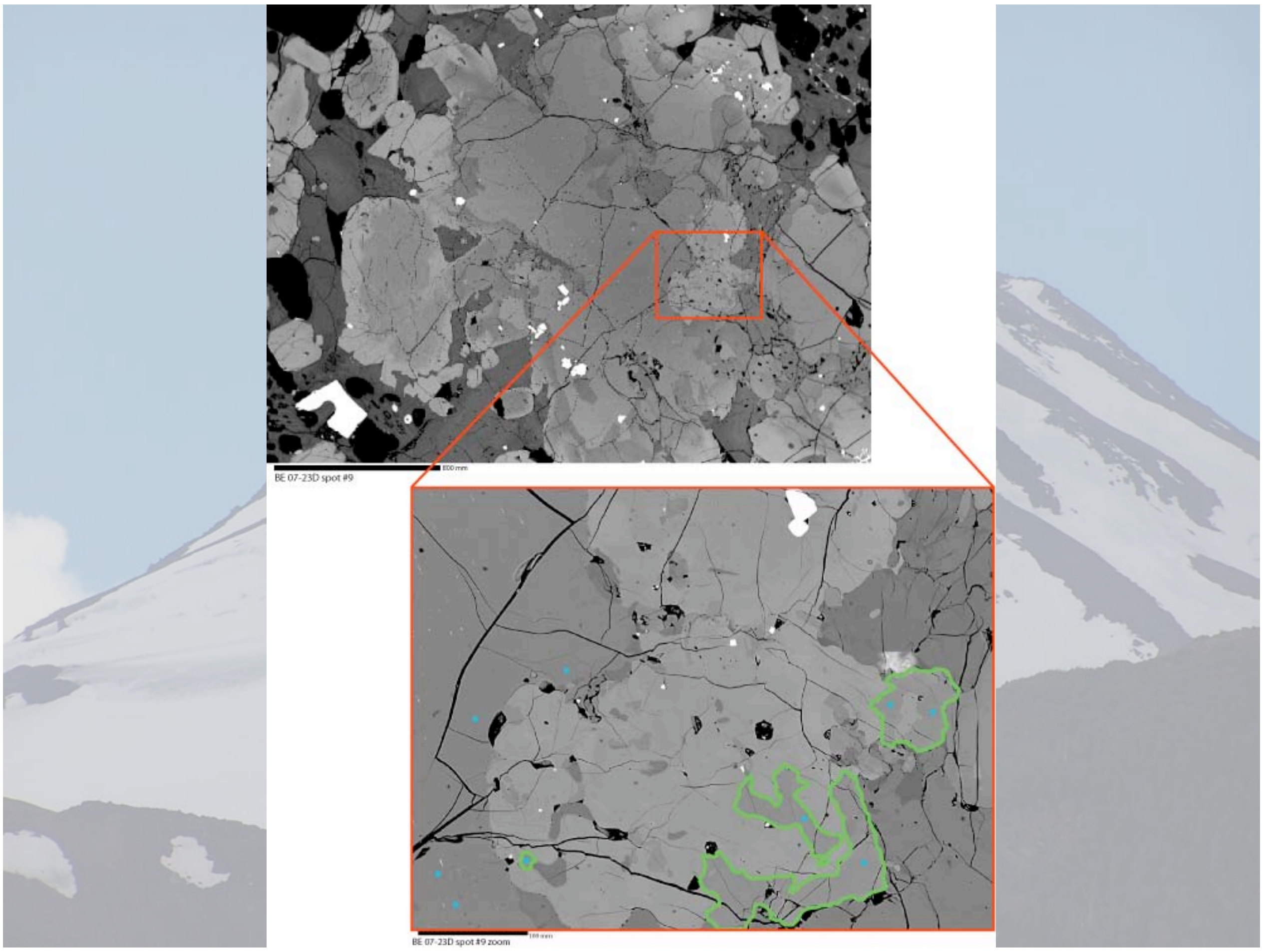
BE 07-23D spot #9
BE 07-23D spot #9 zoom

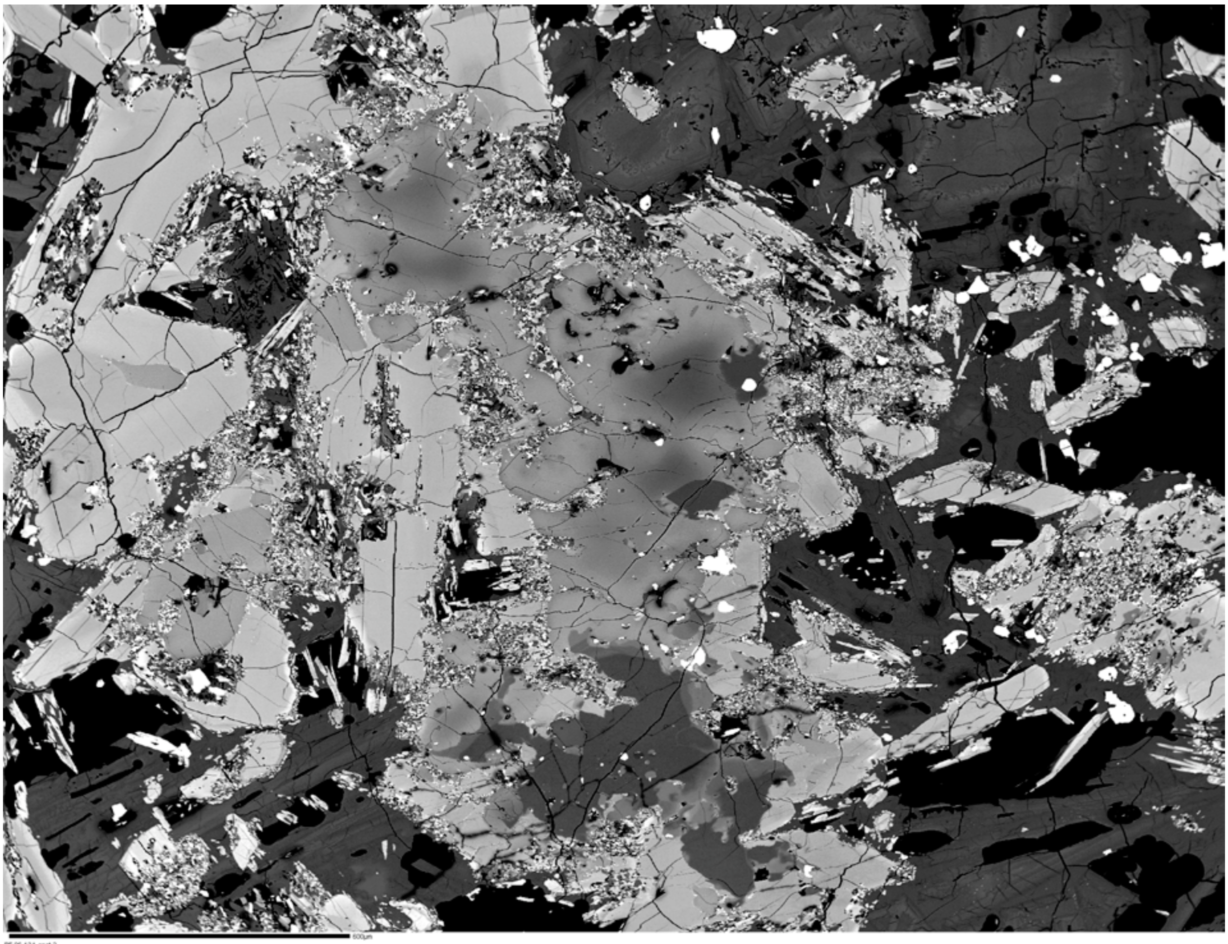
600µm
BE 06-13A spot 2